Brigham and Woman's Hospital/ Harvard Medical School Boston, USA
Department of Translational Medicine
(Director: Thomas P. Stossel, MD)

and

University of Veterinary Medicine Vienna, Austria
Department of Animal Breeding and Reproduction
Institute of Animal Breeding and Genetics
(Director: Univ. Prof. Dr. Mathias Müller)

THE THERAPEUTIC VALUE OF RAPAMYCIN IN A NOVEL MOUSE MODEL FOR TUBEROUS SCELROSIS

Master thesis
submitted to attain the academic grade
'Master of Science'
at the UNIVERSITY OF VETERINARY MEDICINE Vienna

by
Stefanie Anderl
July 2010

Under the external supervision of

David J. Kwiatkowski, MD, PhD and **June Goto, PhD**
Department of Translational Medicine
Brigham and Woman's Hospital/ Harvard Medical School Boston

and the internal supervision of

A. Prof. Dr.rer.nat. Marina Karaghiosoff
Institute of Animal Breeding and Genetics
University of Veterinary Medicine Vienna

I hereby certify that the work presented in this thesis is my own and that work performed by others is appropriately cited.

Hiermit versichere ich, diese Arbeit selbstständig verfasst und andere als die angebenden Quellen und Hilfsmittel nicht benutzt zu haben.

_____

Stefanie Anderl
Boston, July 2010

TABLE OF CONTENT

1 INTRODUCTION 7
1.1 The Tuberous Sclerosis Complex (TSC) 7
1.1.1 Disease, Symptoms and Diagnosis 7
1.1.2 TSC Genetics 8
1.1.3 Tuberous sclerosis and the mTOR pathway 9
1.1.4 TSC Genes and Tumor Development 12
1.2 Rapamycin and the effect in mammals 13
1.3 Animal Models for TSC 15
1.4 The Cre-lox technology for generating mouse models 16
1.4.1 Mouse Models for TSC 16
1.4.2 Mouse Brain Models 17
1.5 The *Tsc1*^{cc} *Nes-Cre*$^{+}$ Mouse Model and the Aim of the Study 19
2 MATERIALS AND METHODS 20
2.1 MATERIALS 20
2.1.1 Chemicals and Reagents 20
2.1.2 Enzymes and Envision Kits 21
2.1.3 Standard Buffer 21
2.1.4 DNA-Isolation, Agarose-Gel Electrophoresis 22
2.1.5 Primer for Genotyping 22
2.1.6 Solutions for Brain Lysates and Western Blotting 23
2.1.7 Solutions for Immunohistochemistry 23
2.1.8 Antibodies 24
2.1.9 Frozen sections and β-Gal staining 25
2.1.10 Solutions for Mouse Treatment 25
2.1.11 Apparates and other Tools 26
2.1.12 Software 26

2.2 METHODS 26
2.2.1 Mouse Procedures and Drug Protocols 26
2.2.2 Rapamycin level measurements in tissue lysates 28
2.2.3 Blood tests 28
2.2.4 DNA isolation and analysis 28
2.2.5 Histology and Immunohistochemistry 30
2.2.6 Immunoblotting / Western Blot Analysis 31
2.2.7 Cell size Measurements 31
2.2.8 Statistics 32
3 RESULTS 33
3.1 Mouse breeding & MLPA analysis to get *Tsc1*^{cw} *Nes-Cre*$^{++}$ parents, which accelerates the breeding for getting *Tsc1*^{cc} *Nes-Cre*$^{+}$ mutants 33
3.2 Organs and tissues in which Tsc1 recombination occurs in *Tsc1*^{cc} *Nes-Cre*$^{+}$ mice 34
3.2.1 Embryonic day E16.5-17.5 34
3.2.2 Postnatal Day 2 34
3.3 Pre- and postnatal Rapamycin Treatment 35
3.3.1 Survival 35
3.3.2 Efficiency of postnatal treatment on lactating mothers 36
3.4 Characterization of the mouse model and effects of Rapamycin in newborn mutant mice 37
3.4.1 Increased Brain/Body Weight Ratio 38
3.4.2 Disorganized Layer formation and enlarged neurons in the motor cortex 39
3.4.3 Hippocampus formation 41
3.4.4 Western Blot and IHC for protein analysis 41
3.5 Further investigations on newborn untreated *Tsc1 cc Nes-Cre*+ mice 43
3.5.1 Kidney 43
3.5.2 Blood 44
3.6 Phenotypic characterization of treated *Tsc1*^{cc} *Nes-Cre*$^{+}$ mice 46
3.6.1 Protein expression levels at the age of P21 and P28 47

3.6.2 Histopathology of treated *Tsc1^{cc} Nes-Cre^{+}* mice at the age of 21 and 28 days 48
3.6.3 Side effects of Rapamycin treatment 51
3.6.4 Control mice and dose effect of *Tsc1* recombination 52
4 DISCUSSION & FUTURE PERSPECTIVES 53
4.1 Breeding 53
4.2 Pre- and postnatal Rapamycin treatment in a severe mouse model for tuberous sclerosis 53
4.3 Characterization of the *Tsc1^{cc} Nes-Cre^{+}* mouse model at P0 56
4.4 Impact of prenatal Rapamycin on *Tsc1^{cc} Nes-Cre^{+}* mice at P0 57
4.5 Advantages and Disadvantages of the *Tsc1^{cc} Nes-Cre+* mouse model 58
4.6 Future Perspectives and planned experiments 59
4.6.1 Dosage, Timing and Effectiveness of Rapamycin treatment 59
4.6.2 Breathing abnormalities in newborn mutant mice 60
4.6.3 mTOR and Hif-1 alpha 63
4.6.4 Blood tests 64
4.6.5 Behavioral studies 65
4.7 Impact of Rapamycin on *Tsc1^{cc} Nes-Cre+* mice and therapeutic values for patients 66
5 ZUSAMMENFASSUNG 67
6 SUMMARY 69
7 REFERENCES 71
8 ABBREVIATIONS 78
9 ACKNOWLEGDEMENTS 79
10 COOPERATIONS 80

1 INTRODUCTION

1.1 The Tuberous Sclerosis Complex (TSC)

1.1.1 Disease, Symptoms and Diagnosis

Tuberous sclerosis complex (TSC) is an autosomal dominant disorder with an incidence of one in 6000 at birth, in which multiple organs systems are affected by benign tumors termed harmatomas. The majority of cases, although, are thought to be due to sporadic mutations without any family background. Any human organ system can be affected whereas most of the pathologies are seen in brain, skin, kidney, heart and lungs. The neurological effects are particularly devastating causing a variety of lesions and symptoms. Most common features of TSC seen in histopathology of the brain are cortical tubers subependymal nodules (SENs) and subependymal giant cell astrocytomas (SEGAs). Generally they are characterized by a disorganization of the layer arrangement seen in the cortex, development of hyperplastic neurons called giant cells and astrocytosis. Cortical tubers are present in 80% of the patients, usually remain during the whole life and do not become malignant. 90% of the patients diagnosed with TSC develop epilepsy and suffer from frequent seizures which are still intractable in some patients and display a major problem in the treatment of TSC. Another main neurological manifestation is developmental delay and behavioral disabilities which are described as autism spectrum disorders and seem to be related to the occurence of cerebral cortical tubers and subependymal nodules. Additional features of TSC are dermatologic manifestations, renal angiomyolipomas and pulmonary lymphangiomyomatosis. Skin lesions such as facial angiofibromas and hypopigmented macules are seen in 90% of affected persons. Renal angiomyolipomas are benign tumors that consist of abnormal blood vessels, fat cells and immature smooth muscle cells and appear in the majority of patients. The abnormal vascular constitution often leads to spontaneous bleeding and life-threatening complications especially when the tumor reaches a certain dimension. Lymphangioleiomyomatosis (LAM), a pulmonary manifestation, only affects adolescent women and is characterized by a proliferation of abnormal smooth muscle cells and cysts within the parenchym of the lung. Besides brain and renal abnormalities these lesions are the third most frequent causes of deaths among TSC patients. In

general the severity of the disease pattern is extremely variable and many patients have minimal symptoms and no neurological disabilities (reviewed by CRINO et al., 2007).

Cortical tubers develop early in embryonic development between 14th and 16th week of gestation. It can be diagnosed prenatally in families with a history of TSC but the disease is mostly detected in early childhood with the occurrence of first neurological symptoms like seizures or cardiac rabdomyomas. Cardiac rabdomyomas are mostly seen in young children and mostly disappear when the person get older. In adults either dermatologic features, renal or lung involvement leads to diagnosis. Dependent on the severity of the disease and the location of lesions patients are currently treated with antiepileptic drugs and removal of cortical tubers that can reduce the frequency of seizures. In some cases transplantation of kidneys or lungs are necessary. Still the therapy can only target specific symptoms and lesions because the genetic and molecular mechanism for initiation and formation of lesions are not fully understood (KWIATKOWSKI, WHITTENMORE and THIELE, 2010).

1.1.2 TSC Genetics

Genomic alterations in the tumor suppressor genes *TSC1* or *TSC2* gene have been shown to be responsible for TSC (KWIATKOWSKI and MANNING, 2005). Even though TSC can be inherited in an autosomal dominant manner, the majority of the cases are thought to be due to sporadic mutations without any family history. *TSC1* is located on chromosome 9q34, contains 23 exons and encodes a 130kDa protein named hamartin. *TSC2* was mapped by positional cloning to chromosome 16p13, is composed of 42 exons and encodes tuberin, a 198kDa protein. Hamartin and tuberin are involved in the mTOR (mammalian target of rapamycin) signaling pathway that is crucial for growth, survival, proliferation and motility of cells. Interspecies comparison showed orthologues of both genes in primates with a 98-99% protein sequence identity for TSC1 and 97-98% identity for TSC2. Other mammals like mouse, rat and dog were sequenced and the amino acid identity ranges from 86-90% for *TSC1* and 91-92% for *TSC2*. Even non-mammalian animals have orthologues to *TSC1* and *TSC2* and especially the coding region of the GTPase activating protein domain (GAP-domain) in *TSC2* seems to be highly conserved among species. The GAP-domain is a functional subunit which is important to regulate downstream proteins connected to the mTOR pathway, which is a conserved pathway regulating cell size and growth (ASTRINIDIS and HENSKE, 2005; INOKI et al., 2005; KWIATKOWSKI and MANNING, 2005). The GAP-domain functions directly against the small

G-protein Rheb (Ras homologue enriched in brain), which is a relatively unique member of the ras family and an important regulator of mTOR (KWIATKOWSKI, WHITTENMORE and THIELE, 2010). Mutations can be detected in one or the other gene and are present in 85% of the patients. The remaining TSC cases are probably caused by mosaicism, by undetected mutations or by the existence of a third unknown locus involved in TSC. Nonetheless patients in which no mutations are found the occurrence of TSC proceeds in a milder way (CRINO et al., 2007). Extensive studies of the two TSC genes in patients have revealed a wide spectrum of different mutations and more than 1500 mutations in *TSC1* and *TSC2* have been reported and collected in the *TSC1/TSC2* database (http://chromium.liacs.nl/LOVD2/TSC/home.php). Sequence variants described include all different kinds of mutations: insertions, deletions, nonsense mutations, splice site variants, point mutations and deletions of larger parts of the gene. Most of the mutations especially frame shift mutations which change the protein sequence and its function show a definite adverse effect (LANGKAU et al., 2002). However there are many mutations in which the reading frame is conserved and the disease causing impact is less clear. The distribution of mutations is not restricted to specific areas in either gene. In *TSC1* a quarter of all of mutations occur in exon 15 because of its relatively large size and exons 8, 17 and 18 show the highest density of mutations. In *TSC2* we see the highest number of mutations in exon 16, 33 and 40 whereas the latter has the highest density of mutations. The alternatively spliced exons 25 and 31 show no functional limitations of the protein. The distribution of mutations seems to reflect the mutability of the sequence itself not the connection to a specific site. Generally *TSC1* mutations account for 21% of all TSC mutations whereas *TSC2* mutations account for about 74%. Differences in the structure of the gene may contribute to the difference in the observed mutation rate. The coding region of the *TSC2* gene is 1.5 times larger that the *TSC1* coding region and there are twice as many splice sites that can be affected. Furthermore missense and large genomic mutations are more common in *TSC2* but rarely seen in *TSC1* (KWIATKOWSKI, WHITTENMORE and THIELE, 2010).

1.1.3 Tuberous sclerosis and the mTOR pathway

On a molecular level TSC1 and TSC2 proteins form a physical and functional complex in which TSC2 functions to accelerate the conversion of the small G protein Rheb (Ras homolog enriched in brain) from GTP to GDP state. Rheb is the major downstream target of TSC1/TSC2 complex and Rheb-GTP binds and activates the mTOR kinase complex which leads cell enlargement and

protein synthesis by phosphorylation of several downstream effectors. The TSC1/TSC2 complex inhibits mTOR indirectly by inactivating the Rheb protein (KWIATKOWSKI 2003).

The mTOR pathway is part of a signaling network that contains a number of tumor suppressor genes including PTEN, LKB1, TSC1, and TSC2, and a number of proto-oncogenes including PI3K, Akt, and eIF4E. It has been shown that mTOR signaling is constitutively activated in many tumor types (LAW, 2005). Mutations in PTEN and LKB1 are associated with other hamartomtous syndromes such as Cowden's syndrome and Peutz-Jeghers syndrome respectively, which show some overlapping pathologies seen in TSC (SHACKELFORD et al., 2009).

The mTOR protein complex consists of a serine-threonine kinase, mTOR (mammalian Target of Rapamycin) and other evolutionary conserved proteins and promotes cellular anabolism in a response to nutrients and growth factors such as amino acids, glucose and insulin. mTOR exists in two distinct multi-protein complexes termed as mTORC1 and mTORC2 (mTOR complex 1/2) whereas only mTORC1 is sensitive to rapamycin, a fungal metabolite (figure 1). In yeast, TOR kinases are encoded by two different genes TOR1 and TOR2 and have distinct functions. However in higher eukaryotes there is only one TOR gene but two distinct protein complexes (INOKI and GUAN, 2009). mTORC1 suppresses the binding of 4EBP to eIF4E protein by phosphorylating 4EBP. Hence eIF4E, a translation initiation factor important for overall translation in cells, gets activated. It enhances proliferation, survival and angiogenes by phosphorylating downstream effectors that lead to selective expression of cyclines, vascular endothelial growth factor (VEGF) and Bcl-genes that are known to inhibit apoptosis. mTORC1 also activates S6K, which regulates cell growth by phosphorylating ribosomal proteins, insulin receptor substrate 1 (IRS-1) and other cell growth connected proteins (MERIC-BERNSTAM and GONZALEZ-AGULO, 2009).

mTORC2 is insensitive to nutrients or energy conditions. However, in response to hormones or growth factors, mTORC2 phosphorylates Akt, and regulates cell survival. Another major role is the regulation of actin cytoskeleton through phosphorylation of PKCα, Rho and Rac, (SOULARD and HALL, 2007) shown in figure 1. In contrast to mTORC1, mTORC2 is not sensitive to Rapamycin. It does not bind to mTORC2 or affects its function directly. Instead, by promoting rapamycin-FKBP12-mTORC1 complex, rapamycin can bind up all free mTOR molecules, leading to depletion of mTORC2 (SARBASSOV et al., 2006). Because of the availability of rapamycin which selectively inhibits mTORC1 there has been more progress in

understanding the activity and functions of mTORC1. In TSC1/ TSC2 mutant cells and organisms the mTOR1 pathway is constitutively active. Due to lack of TSC1/TSC2 complex the Rheb protein cannot be converted to its GDP state and permanently activates the mTORC1 complex. The best characterized mTORC1 function is its involvement in protein synthesis especially the translation of proteins responsible for cell growth. In addition mTORC1 activation stimulates mitochondrial metabolism and biogenesis, ribosomal biogenesis and negatively regulates autophagy. Therefore hyperactivation of mTOR1 has been shown to be a contributing factor in tumorigenesis (INOKI and GUAN, 2009).

The TSC1/TSC2 complex itself is regulated by upstream signals that are connected to the available energy levels inside and outside the cell. Under energy starvation conditions, the AMP-activated protein kinase (AMPK), which is a sensor for intracellular energy levels, phosphorylates TSC2 at Ser1345 and enhances its activity. Phosphorylation of Ser1345 of TSC2 by AMPK is required for translation regulation and cell size control in response to energy deprivation (INOKI et al., 2003) Growth factors like insulin from outside the cell activate the protein kinase B/AKT and ERK that inhibits TSC1/TSC2 function by phosphorylating Ser939 and Thr1462 of TSC2 (INOKI et al., 2002) and thus increases protein synthesis and stimulates cell growth.

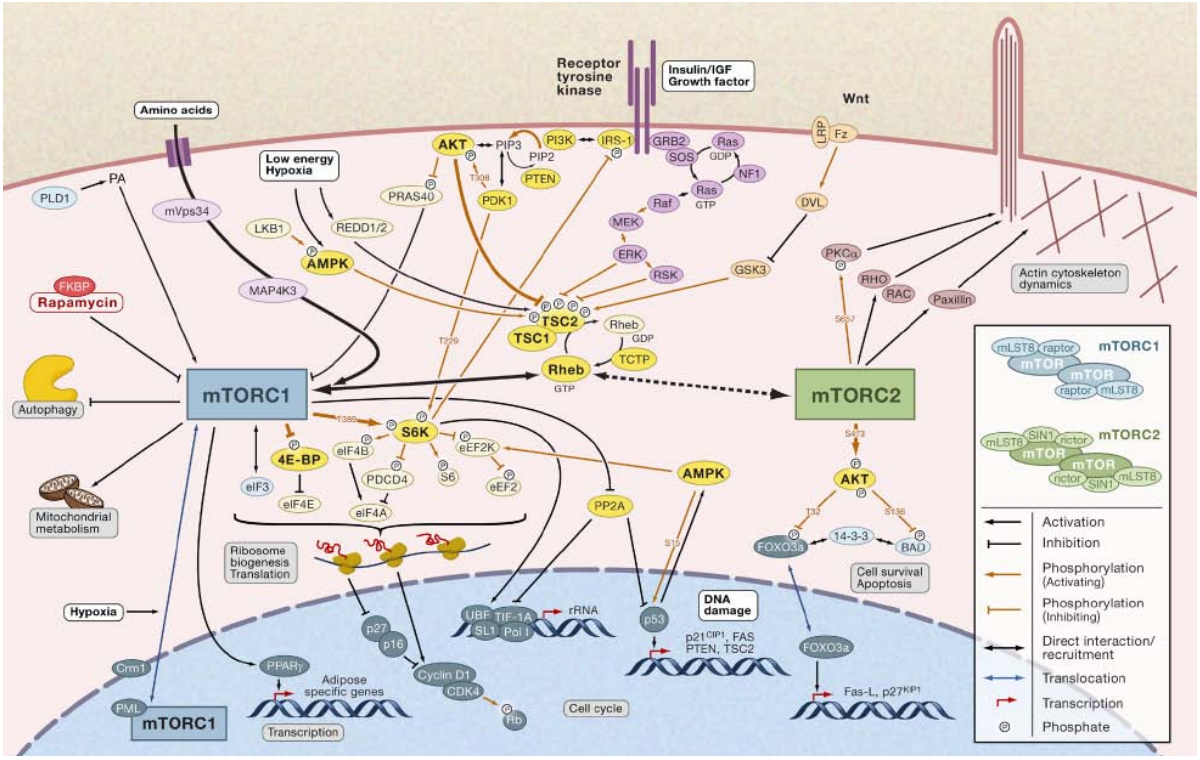

Figure 1: TSC proteins and the mTOR pathway (Alexandre Soulard and Michael N.Hall, Cell 129, April 20, 2007)

1.1.4 TSC Genes and Tumor Development

Although TSC is a dominant disorder, mutations in the TSC genes are recessive on the level of the affected cell and lead to their classification as tumor suppressor genes (HENGSTSCHLÄGER 2001). The current model for tumor development in TSC patients is the so called two hit model. It postulates that in hamartomas and other TSC lesions loss of the second unaffected *TSC1* or *TSC2* allele is combined with the loss of the first allele by germline mutation leads to complete loss of either TSC1 or TSC2 protein. The second hit loss might occur through different genetic and epigenetic mechanisms, but the most common event is a large deletion which can be detected by the screening for loss of heterozygosity (LOH) with the use of genetic marker (KWIATKOWSKI, WHITTENMORE and THIELE, 2010). LOH has been consistently reported in TSC-associated angiomyolipomas, cardiac rhabdomyomas, subependymal giant cell tumors and lymphangiomyomatosis but is only rarely detected in cortical tubers (CRINO et al., 2006).

The mTOR pathway is thought to be involved in cancer development in most patients. The PI3K/PTEN/AKT pathway has been shown to be activated in the majority of human cancers. The TSC1/TSC2 complex is downstream of AKT where TSC2 is directly phosphorylated and inactivated by AKT (KNOWLES et al., 2009) and the TSC complex also integrates signals from other pathways, such as RAS/MEK/ErK to regulate mTOR. Therefore it is highly possible that mTOR contributes to cancer involvement here but clear evidence of direct involvement of loss of TSC1 or TSC2 in common cancers is quite limited. This may be due to the negative feedback mechanism through phosphorylation and degradation of IRS-1 by S6K (figure 1). However, single copy loss of the *TSC1* gene has been reported in several human cancer including bladder carcinoma, ovarian carcinoma, gallbladder carcinoma, nasopharyngeal carcinoma and nonsmall cell lung cancer and may contribute through a haploinsufficiancy mechanism to tumor development (KWIATKOWSKI, WHITTENMORE and THIELE, 2010).

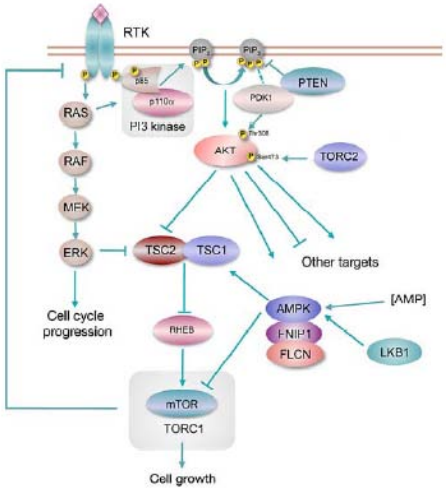

Figure 2:PI3K/PTEN/AKT pathway network and connection to Tsc1/2 and the mTOR (Knowles et al., 2009)

1.2 Rapamycin and the effect in mammals

Rapamycin, also known as Sirolimus is a bacterial metabolite and was first isolated from the bacterium *Streptomyces hygroscopicus* found on Rapa Nui the Easter Island in the parcific ocean (VEZINA et al., 1975). It is a commercially available drug widely used as an immnosupressant in transplant patients. Rapamycin binds to FKBP12 (FK506 binding protein 12 kDa), a member of the protein family immunophilins, the FKBPs. The complex inhibits mTOR, which phosphorylates proteins involved in cell cycle and therefore plays a cirical role in transmitting signals to stimulate lymphocyte proliferation. (TEPPERMAN et al., 2010). Rapamycin blocks the activation of T-effector cells by inhibiting the response to IL-2 which is crucial for activating these cells. Recently rapamycin was also shown to selectively expand the T-regulator cell population. CHEN et al. 2010 showed that rapamycin can convert peripheral naïve T-cells to T regulator cells using B cells as antigen presenting cells. This subtype of Treg cells can potently suppress T effector cell proliferation and maintain antigenic specificity. This finding provides evidence for another mechanism for tolerance induction by rapamycin.

The complex of rapamycin and FKBP12 protein inhibits mTOR kinase activity only when mTOR is present in mTORC1. Since mTOR has been shown to be constitutively active when there is a mutation in *TSC1* or *TSC2,* mTOR inhibitors are a new treatment options for TSC and seem to be promising in preliminary rapamycin studies in TSC patients (FRANZ et al., 2006 and BISSLER et al., 2008). In addition different derivates of rapamycin have been used in clinical studies like RAD001 (everolimus) and CC1-779 (temsirolimus) a prodrug from rapamycin. Those derivates act in a similar fashion as rapamycin but pharmacokinetics, bioavailability and side effects may differ (FRANZ et. al, 2006).

The positive effect of rapamycin has been already shown in several mouse models for TSC in reversing epileptic phenotypes, improving survival rate (Meikle et al., 2008; Zheng et al.,2010) and arrest tumor growth in renal angiomyolipomas in the Eker rat (FRANZ et al., 2006). Those aspects are described in chapter 2.3 in more detail.

In the study from FRANZ et al., 2006, rapamycin has been shown to be effective in 5 patients with SEGAs, which is seen in 5-15% of TSC patients and induce significant neurological effects due to the production of hydrocephalus, mass effect and their characteristic position near the foramen of Monro (small opening that connects the third ventricle with the lateral ventricle). Resection is the usual treatment for large SEGAs that are causing hydrocephalus and that have

grown significantly. Oral rapamycin treatment with a standard immunosupressive dose (5-15ng/ml serum) for several months lead to a regression of SEGAs in all patients. Interruption of rapamycin treatment led to regrow of the lesion in one patient. These findings are preliminary considering the low numbers of patients tested, but results it strongly highlights the efficacy of rapamycin in this particular manifestation of TSC (FRANZ et al., 2006).

Targeting the mTOR pathway is also thought to be beneficial in other human cancers. In a clinical trial phase III patients with advanced renal cell carcinoma were treated with temsirolimus, interferon or a combination of the two drugs. Patients who received temsirolimus alone showed a significantly higher overall survival rate than patients who got interferon alone. In the combination group the overall survival did not differ much from the interferon group. Rapamycin analogs have been tested in other cancer types and show clear activity in lymphomas, showed regression in Kaposi's sarcoma in renal transplant patients and seem to be promising in the treatment of sarcoma and endometrial cancer. Although rapamycin alone failed to show any appreciable single agent activity in many other cancer types, the overall cytostatic impact may be useful in combination treatment and a stabilizing factor of disease. (MERIC-BERNSTAM and GONZALEZ-AGULO, 2009)

However, rapamycin does not have a cytotoxic effect on cancer cells and the inhibition of mTOR sensitizes the PI3-K/Akt pathway to growth factors. It also enhances autophagy, a catabolic cellular process to provide nutrients, degrading cell organelles and proteins during starvation. These facts suggest that rapamycin might act by causing inhibition of cell growth, and cell size reduction, without induction of cell death. These effects might still be beneficial, but could suggest that lifelong treatment would be necessary. There are new approaches in combining mTOR inhibitors with either inhibitors of receptor tyrosine kinases for growth factors or PI3K or autophagy inhibitors. A major problem with testing therapeutic approaches is the current lack of preclinical animal models that display manifestations of TSC comparable to TSC patients (KWIATKOWSKI, WHITTENMORE and THIELE, 2010).

Recently rapamycin was shown to extend life span in mice even when administered late in life (HASTY 2010). Because mTOR is known to be a master regulator in protein synthesis and cell growth and caloric restriction in general increases life span in a wide range of species, it is possible that a chemical intervention that inhibits cell growth pathways and protein synthesis may also lead to extended life span. Side effects of rapamycin could be more severe given in

early stages of development when growth is important for fitness. Later in life growth is less important and even seems to provide age related diseases (HASTY, 2010). Although treating patients early in life with rapamycin could be harmful from the point of view of growth and development, there may also be benefits from early treatment, such as reduction of symptoms seen in TSC. Therefore, the goal of this study is to investigate the impact of prenatal rapamycin treatment in combination with postnatal treatment on a new mouse brain model of TSC.

1.3 Animal Models for TSC

The first animal model was due to a spontaneous *Tsc2* mutation in the rat that was first described as an autosomal dominant predisposition to renal carcinoma named after Eker (EKER 1954). Investigation on the Eker rat has first shown that the *Tsc2* gene acts like a tumor suppressor gene and tumor development occurs due to a germline inactivation of one *Tsc2* allele followed by the loss of the other allele by a second-hit event in the affected tissue. Furthermore studies on the Eker rat has revealed the existence of genetic modifiers in different rat strains that influence the tumor size. Furthermore pathway studies showed expression of mTOR1 activation markers restricted to tumor lesions. These aberrant expression patterns could be compensated by rapamycin treatment (KENERSON et al., 2002).

Since many important signaling pathways are highly conserved even in evolutionary distant species, it is possible to investigate basic molecular mechanisms of human disease genes in the widely used animal model *Drosophila melanogaster*. Studies in Drosophila mainly led to the understanding of molecular mechanism of the TSC1-TSC2 tumor suppressor complex, the connection to the small GTPase Rheb and the Serin/Threonin Kinase TOR and the integration of TSC protein in the Insulin/PI3K signaling pathway (KWIATKOWSKI, WHITTENMORE and THIELE, 2010).

In the last decades though the mouse gained value as a model organism, because as a mammal it is closer to humans and there are powerful and well-engineered methods to manipulate the mouse genome for proper investigation.

1.4 The Cre-lox technology for generating mouse models

The Cre-lox system is a technique to produce conventional knockouts, conditional knockouts and reporter strains of animal models (http://cre.jax.org/introduction.html). It was first discovered in P1 bacteriophage as part of the normal viral life circle (SAUER and HENDERSON, 1988). The virus uses Cre-lox recombination to circularize and allow the replication of its genomic DNA during reproduction. Since the discovery this system has been used as a powerful tool for genome manipulation and was successfully applied to mammalian cells, yeast, plants, mice and other organisms. The Cre-recombinase is an enzyme that catalyzes recombination between two specific 34 basepair sequences called lox-P sites. Because the Cre-recombinase and similar sequences to the lox-P sites are not present in the mouse genome, one can manipulate those sequences to introduce them into the desired position of the mouse genome by transgenic methods. Dependent on the orientation of the lox-P sites translocation, insertion or deletion can be induced (SAUER, 1998)

In case of the multi organ disease TSC, the Cre-lox system appeared to be a suitable tool to generate mouse strains with tissue specific loss of one of the two *Tsc* genes. Using different promoter-driven Cre-recombinases not only the tissue specificity but also the time of recombination during development can be established. It has been shown that homozygousity in conventional knockout of either Tsc1 or Tsc2 causes early embryonic death and heterocygositiy of either Tsc1 or 2 genes do not show any brain pathology similar to TSC patients (KWIATKOWSKI, WHITTENMORE and THIELE, 2010). Therefore, the usage of Cre-lox systems became an indispensable method to overcome these problems and develop mouse brain models for tuberous sclerosis.

1.4.1 Mouse Models for TSC

For *Tsc1* as well as for *Tsc2* knockout (null/-) alleles have been generated (4 Ref from book). *Tsc1*$^{+/-}$ and *Tsc2*$^{+/-}$ animals develop kidney tumors by 6-12 months, liver hemangiomas and hemangiosacromas on tail, mouth and paws, but no brain lesions have been observed in both models. Consistent with the two hit model, loss of the second wild type allele has been detected in those lesions (KOBAYASHI et al., 1999; ONDA et al., 1999; KOBAYASHI et al., 2001; KWIATKOWSKI et al., 2002)

Furthermore, *Tsc2*$^{+/-}$ mice show moderate impaired spatial learning and deficits in memory which can be reversed by rapamycin. These results support a possible haploinsufficiency model for the path of neurological symptoms in patients (EHNINGER et al., 2008).

With the usage of tissue specific Cre alleles and conditional *Tsc1* and *Tsc2* alleles other mouse models for specific lesions in TSC have been generated.

1.4.2 Mouse Brain Models

Due to the fact that neurological traits of TSC are the most destructive and most difficult to treat in humans there is acute interest to understand and treat the brain manifestation of this disease. Conventional knock-out mice for *Tsc1* and *Tsc2* are not viable. Therefore several groups tried to establish mouse models mainly using Cre-lox technologies to generate similar neurological pathologies as seen in TSC patients.

1.4.2.1 The *Tsc1cc Synapsin-Cre* Mouse Model – cortical giant cells and seizures

In this model a floxed conditional *Tsc1* allele was used as previously described above (KWIATKOWSKI et al., 2002) and consequently combined with a synapsin-Cre-recombinase allele (MEIKLE et al., 2008). In *Tsc1*$^{c-}$*Syn1Cre*$^{+}$ mice, the expression of Tsc1 is inhibited in most neurons beginning around embryonic day 13 (E13). The synapsin promoter leads to expression of Cre recombinase in brain progenitor cells as they begin to differentiate into neurons. Recombination at the *Tsc1* conditional locus leads to loss of several exons of the gene, and complete loss of Tsc1 expression in the vast majority of neurons in these mice. *Tsc1*$^{c-}$ *Syn1Cre*$^{+}$ mice show delayed development beginning at postnatal day 5 (P5), spontaneous seizures and a median survival of 35 days. Many cortical and hippocampal neurons are ectopic, enlarged and aberrant which are similar to dysplastic neurons seen in cortical tubers of TSC patients. Those neurons show a higher expression of phsopho- S6, that indicates a strong activation of the mTOR pathway. Additionally a delay in myelination is seen which can be a neural defect in induction and interaction with oligodendrocytes. Rapamycin treatment given intraperitoneally starting at P7-P9 in a dosage of 6mg/kg every other day resulted in a significant improvement of the survival rate to a median survival of more than 80 days with a continuous treatment. As soon as treatment is stopped the survival curve declines within a period of 1-2 weeks. In addition the treatment resulted in an enhancement of myelination resulting in a decrease of seizure frequency. On the other hand rapamycin treated control mice showed a reduced myelination whereas in mutants the hypomyelination could be reversed and led to a

lower seizure frequency (MEIKLE et al., 2008). Since the mTOR pathway is important for normal growth including the development of oligodendrocytes, the dosage and timing of rapamycin treatment is a critical factor to keep side effects as low as possible.

1.4.2.2 The Mouse Model – epilepsia model

Recent studies in human tissue as well as in mouse models of TSC suggest that astrocytes play an important role in epileptogenesis and other neurological deficits in TSC (UHLMANN et al., 2002). In normal brains astrocytes form the blood brain barrier, provide nutrition for neuronal tissue, maintain the extracellular ion balance and are involved in scarring processes. The close contact and the balanced interaction between neuronal and glial cells are essential for the maintenance of physiological brain functions. Furthermore astrocytes are responsible for the regulation of extracellular and synaptic glutamate homeostasis. Accumulation of glutamate in synaptic areas, the major excitatory neurotransmitter in the brain, in synaptic areas is thought to cause excitatory stress on neurons and lead to seizures and neuronal death (WONG et al. 2003). The mouse model described here has a conditional inactivation of the Tsc1 gene in glial cells that is accomplished by the use of the GFAP (Glial fibrillary acidic protein) promoter driven Cre-Recombinase starting around embryonic day 14.5. Knockout mice show a decrease in the expression of GLT-1, an astrocytic glutamate transporter and develop frequent progressive seizure at the age of 3 weeks. The mTOR inhibitor rapamycin as well as Ceftriaxone which is known to increase the level of glutamate receptors have been shown to prevent the neurological phenotype in these mice especially when given before the onset of seizures. This mouse model gives inside in possible mechanisms of astrocyte driven epilepsy in TSC and gives approaches for novel therapies (ZENG et al., 2010).

1.5 The *Nes-Cre*$^{+}$ Mouse Model and the Aim of the Study

Despite all efforts to create mouse brain models for TSC, no brain lesions like cortical tubers, the main pathology seen in patients, could be generated in mice so far. Nestin is an intermediate filament protein that was first found in neuroepithelial cells of the rat and its expression is widely used as a marker for neural stem cells and progenitor cells (DAHLSTRAND et al., 1995). Prior to my arrival in the lab of the mentor, Dr. June Goto in our institute generated *Tsc1cc Nestin-Cre*$^{+}$ mice to examine the effects of loss of Tsc1 from nearly the beginning of brain development. The nestin promoter is known to be expressed in earlier stages of brain development than the synapsin promoter described before. This is thought to be closer to the development of TSC in humans in which tuber-like lesions are seen in early gestation between week 14 and 16. *Nes-Cre* mediated recombination was detected in *Tsc1*^{cc} *Nestin-Cre*$^{+}$ embryos at the earliest stages examined E 7.5-E8 (DUBOIS et al., 2006)

In initial studies *Tsc1*^{cc} *Nestin-Cre*$^{+}$ mice were observed to die short after birth. Originally, this model was generated to establish and investigate glioneuronal hamartomas, the main brain manifestations in TSC. Because of the perinatal death, the emphasis in this project is to investigate the effects and therapeutic values of pre- and postnatal rapamycin treatment and its impact on survival of pups and pregnancy. Since cortical tubers can be detected in patients before birth, prenatal treatment is from relevant interest, as it has the potential to control tuber development from the beginning and improve progression of disease later on in life. Here we demonstrate that rapamycin given prenatally improves the survival in a severe model of TSC and does not interfere with the development and survival of control littermates. Another focus of the presented study is to characterize pathologies in the *Tsc1*^{cc} *Nestin-Cre*$^{+}$ mouse model in newborn animals and compare mutants after rapamycin treatment. We describe possible side effects of rapamycin in addition to the phenotype and histopathology of mutant mice after treatment.

2 MATERIALS AND METHODS

2.1 MATERIALS

2.1.1 Chemicals and Reagents

5-Bromo-4-chloro-3-indolyl-β-D-galactopyranos (X gal), Sigma Aldrich B9146, GER

100 basepair DNA ladder, New England Bio Labs, USA

Agarose NuSieve® 3:1, Lonza, Rockland, USA

Avertin (2,2,2-Tribromoethanol), Sigma Aldrich, GER

Bouins Solution, Sigma Aldrich, GER

Bovine Serum Albumin (BSA), Sigma Aldrich, GER

Bromdesoxyuridin (BrdU), Sigma Aldirch B5002, GER

Citric Acid, Sigma, St.Louis, USA

Deoxychloride Acid (NadOc), Sigma Aldrich,, GER

Dimethylsulfoxide (DMSO), Sigma Aldrich,, GER

dNTPs, New England Bio Labs, USA

EDTA, American Bioanalytical, Natick, USA

Ethidiumbromide, Thermo Scientific, Rockford, USA

Ethyl-Alcohol, Pharmco-Aaper, USA

Gene Amp 10 x PCR Buffer, Applied Biosystems, USA

Hematoxylin, Mayer's Hematoxylin Solution, Sigma Aldrich, GER

Hydrogen Peroxide 30%, Fisher Scientifics, Pittsburgh, USA

Iso Propyl Alcohol, VWR Scientific Products, West Chester, USA

Magnesium Chloride, Sigma Aldrich, GER

Methanol, Fisher Scientifics, Pittsburgh, USA

Nonylphenoxylpolyethoxylethanol (NP-40) = Igepal CA-360, Sigma Aldrich, GER

Nuclear Fast Red, Vector Laboratories Inc., Burlingame, USA

Paraformaldehyde, Boston Bioproducts, USA

Potassium Ferrocyanide Trihydrate, Sigma Aldrich, GER

Potassium Ferrocyanide, Sigma Aldrich, GER

Rapamycin, LC Laboratories,Boston, USA

Sodium Chloride, American Bioanalytical, Natick, USA

Sucrose, American Bioanalytical, Natick, USA

Tris-HCl, American Bioanalytical, Natick, USA

Triton X-100, Sigma Aldrich, GER

Tween20, American Bioanalytical, Natick, USA

Vecta Mount, Permanent Mounting Medium, Vector Laoratories Inc, USA

Vectashield, Mounting Medium with DAPI, Vector Laoratories Inc, USA

Xylene, Fisher Scientifics ID:X3S-4, Pittsburgh, USA

2.1.2 Enzymes and Envision Kits

Ampli Taq Gold, Applied Biosystsems, USA

Proteinase K, American Bioanalytical, Natick, USA

RNAse A, Sigma Aldrich, GER

EnVision+System-HRP (DAB), Dako, DK

HistoMouse™-Plus Kit, Invitrogen

SuperSignal®West Pico Chemiluminescent Substrate, Thermo Scientific,USA

SuperSignal®West Femto Chemiluminescent Substrate, Thermo Scientific,USA

2.1.3 Standard Buffer

	Chemical, Company	*stock*	*final*
TBS (10x Tris Buffered Saline)	Tris-HCl, pH 7.4 NaCl		100 mM 1.2 M
PBS	Boston BioProducts, US	10x	1x

2.1.4 DNA-Isolation, Agarose-Gel Electrophoresis

	Chemical,Company	*stock*	*final*	*amount*	*vol*
TETT-buffer	Tris-HCl, pH 8.3 EDTA Tween20 TritonX-100	2M 500mM 10% 10%	20mM 0.1mM 1% 0.2%	1ml 20µl 10ml 2ml	100ml
Cell lysis solution	Quiagen Sciences, USA				
Protein Precipitation Solution	Quiagen Sciencens, USA				
6x loading dye	Glycerol Bromophenol blue		30% 0.25%	15ml 125mg > 50ml	50ml
20x TAE running buffer	Tris EDTA 0.5M		800 mM 380 mM 20 mM	96.8g 22.8ml 40ml	1l

2.1.5 Primer for Genotyping

Tsc1	F4536	5’ AGGAGGCCTCTTCTGCTACC 3’	Invitrogen
	R4830	5’ CAGCTCCGACCATGAAGTG 3’	Invitrogen
	COR4771	5’ AGCCGGCTAACGTTAACAAC 3’	Invitrogen
Cre-Recombinase	Cre-NesF	5’ TGGGCGGCATGGTGCAAGTT 3’	Invitrogen
	Cre-NesR	5’ CGGTGCTAACCAGCGTTTTC 3’	Invitrogen

2.1.6 Solutions for Brain Lysates and Western Blotting

	Chemical	*stock*	*final*	*amount*	*vol.*
Lysis Buffer (TBSV)	Tris-HCl pH7.5 NaCl NaF (Ser-Thr Inhibitor) (PTPase Inhibitor) EDTA	2M 2.5M 1M 100mM 0.5M	20mM 140mM 10mM 1mM 1mM	100µl 560µl 100µl 100µl 20µl	10ml
Working Solution for 10ml Lysis Buffer	β Glycerol Phosphatase Phosph. Inh. Cocktail P-2850 Phosph. Inh. Cocktail P-5726 Protease Inh. Cocktail P8340	1M	10mM	100µl 100µl 100µl 100µl	
Running Buffer MES-SDS (20x)	MES Tris SDS EDTA	 20%	1000 mM 1000 mM 20 mM	195.2g 121.2g 100ml 7.63g up to 1l	1l
Transfer Buffer (20x)	Bicine Bis-Tris EDTA disoduim dihydrate Chlorobutanol		500 mM 500 mM 20.5mM 1 mM	81.6g 104.64g 7.36g 0.18g up to 1l	1l
Transfer buffer (4x)	20x transfer buffer stock methanol SDS	 20%	1x 20% 0.01%	200ml 800ml 2ml 3l	4l
Blocking Solution	Skim milk Tween20 1x TBS	 10%	3% 0.05%	 > 40ml	40ml

2.1.7 Solutions for Immunohistochemistry

Washing Buffer (TBST)	1xTBS 0.05% Tween20
Blocking Solution	1xTBS 0.05% Tween20 2% normal serum 1% BSA
Citrate Buffer pH 6.0	Dako Target Retrieval Solution 10x Conc. Ref : S1699, Lot : 10021452
Bouins solution	Sigma #HT101128 Formaldehyde 9%, picric acid 0.9%, acetic acid 5%

2.1.8 Antibodies

2.1.8.1 Primary Antibodies for Western Blot

Antibody	*Company*	*Dilution*
Phospho-S6 Ribosomal Protein (Ser235/236) (pS6) #22115 rabbit mAB (91B2)	Cell Signalling Technology Danvers, USA	1:2000
Phospho-S6 Ribosomal Protein (Ser240/244) #22155 rabbit mAB	Cell Signalling Technology	1:2000
TSC1/ Hamartin #4906 rabbit mAB	Cell Signalling Technology	1:1000
TSC2/ Tuberin #SC-893 (C20) rabbit polyclonal IgG	Santa Cruz Biotechnology Santa Cruz, CA	1:2000
Akt1 (C-20) #SC-1618 goat polyclonal IgG	Santa Cruz	1:3000
pAkt (pS473) #M3628 rabbit mAB, anti human	Dako North America Capinteria, CA	1:1000
Myelin Basic Protein (MBP) #AB980 rabbit polyclonal AB	Millipore, Billerica, MA	
Glutamate decarboxylase 67 (GAD67) #MAB351 mouse mAb	Millipore	
Neurofilament #MAB5254 mouse mAb	Chemicon International	1:1000
Protein Kinase c alpha (PKCα) #2056 rabbit mAB	Cell Signaling	1:1000
Pospho-PKCα Ser657 06-822 rabbit mAB	Millipore	1:1000
GFAP # SMI-22	Covance	1:2000

2.1.8.2 Secondary Antibodies for Westernblot

Antibody	Company	Dilution
Goat-anti Mouse IgG-HRP #E0506	Santa Cruz Biotechnology	1:3000
Rabbit-anti Goat IgG-HRP #F1807	Santa Cruz Biotechnology	1:3000
Goat-anti Rabbit IgG-HRP #J3108	Santa Cruz Biotechnology	1:3000

2.1.8.3 Primary Antibodies for Immunohistochemistry (IHC)

Antibody	*Company*	*Dilution in blocking solution*
Phospho-S6 Ribosomal Protein (235/236) (pS6) #2211L rabbit mAb Lot:3 (IHC)	Cell Signalling Technology	1:1000
PCNA #PC10 sc-56 FITC conj., mouse mAb	Santa Cruz	1:500
GFAP Rabbit pAb (whole antiserum) #7260-50	Abcam	1:5000

For the color reaction in IHC the DakoCytomation EnVision+System-HRP (DAB) – Kit for rabbit primary antibodies was used in which the secondary antibody is labeled with Horse-radish peroxidase and envisioned with DAB (3,3´-diaminodbenzidine) -substrate.

2.1.9 Frozen sections and β-Gal staining

	Chemical	*stock*	*final*	*amount*	*vol.*
Frost protection	sucrose in 1xPBS		30%		
Post fixation	PFA in 1xPBS		0.2%		
lacZ staining solution	phosphate buffer pH 7.3 NadOc (Deoxychloric Acid) NP-40 (Igepal) Potassium Ferrocyanide Trihydrate Potassium Ferrocyanide Tris pH 7.5 Xgal in DMF (Dimethylfuran)	0.5 M 1M 10% 10% 2M 20mg/ml		8 ml 80 µl 40 µl 80 µl 0.06 g 0.08 g 0.4 ml 1 ml 29.4 ml	40ml
lacZ detergent rinse	phosphate buffer pH 7.3 NadOc NP-40	0.5 M 1M 10% 10%		40 ml 0.4 ml 0.2 ml 0.4 ml 159 ml	200ml

2.1.10 Solutions for Mouse Treatment

2.1.10.1 Stocks

Rapamycin in EtOH	20 mg/ml		final
Sterile Vehicle		2.5 ml of 5% PEG 2.5 ml of 5% Tween 20 45 ml	0.25% 0.25%

2.1.10.2 Working solutions

Concentration	Rapamycin	Vehicle	Weight of mouse
1mg/kg	3 µl	200 µl	60 g
3mg/kg	9µl	200 µl	60g
6mg/kg	18µl	200 µl	60g

2.1.11 Apparates and other Tools

Centrifuge 5415D, Eppendorf

Leica CM 3050S, Cryostat, Leica

PTC-100™ Programmable Thermal Controller, PCR machine, MJ Research Inc.

Ulrtospec 2000, UV/ visible Spectrophotometer, Pharmacia Biotech

HEMAVET®850, blood count system, CDC Technologies Inc.

One Touch Ultra Mini®, Blood Glucose Monitoring System, Johnson-Johnson

Syngene (G:BOX) envision system

Heparinized Micro-Hematocrit Capillary Tubes, Fisher Scientific

Nikon Eclipse E400 Brightfield Microscope

2.1.12 Software

Prism 4

Image J

Exel, Word, Powerpoint

2.2 METHODS

2.2.1 Mouse Procedures and Drug Protocols

As mentioned before in the introduction mouse experiments were performed on a mixed genetic background (C57BL/6, 129/SvJae, BALB/c) to generate the combination of alleles required. Those are the Tsc1 condidional allele, the nestin promoter driven cre-recombinase and the Rosa 26 vector driven beta-galactosidase reporter allele (SORIANO 1999). Mice carrying the Nestin driven cre recombinase derived from the congenic mouse strain B6.Cg-Tg(Nes-cre)1Kln/J which was obtained from Jackson Laboratories. These transgenic mice express cre-recombinase under the control of the rat nestin promoter. The nestin promoter is known to be specific for its activity in neuronal progenitor cells although lower expression sites have been found in several other

tissues (http://cre.jax.org/Nes/Nes-Cre.html, TRONCHE et al., 1999). Hemizygous and homozygous mice for this transgenic insert are viable, fertile and do not show any severe behavioral abnormalities. (http://jaxmice.jax.org/strain/003771.html).

In addition mice carrying the floxed β-galactosidase reporter allele (B6.129S4-Gt(ROSA)26 Sor^{tm1Sor}/J) were obtained from Jackson Laboratory. The expression of this allele is dependent on the cre-mediated recombination. In presence of the cre-recombinase the floxed stop sequence, which blocks β-galactosidase expression, is removed and beta-galactosidase expression is induced. This can be visualized by an enzymatic reaction that produces a blue stain in lightly fixed frozen sections. Previous studies with β-gal allele showed that Nestin-Cre is mainly expressed in the central and peripheral nervous system and in a few isolated kidney and heart cells. The cre-recombinase activity starts at embryonic day 8.5 in the nervous tissue.

In *Tsc1^{cc} Nes-Cre^{+}* mice the nestin promoter driven cre-recombinase allele initiates the recombination of exon 16-18 of the Tsc1 conditional allele. Exons 16-18 are flanked by loxP sites that function as cre recognition sites.

The Tsc1 conditional allele was generated as described previously by using gene targeting including 129/SvJae stem cells and BALB/c mice as recipients (KWIATKOWSKI et al., 2002). Mutant mice were generated by breeding *Tsc1^{cc}Nes-Cre^{-}* females to *either Tsc1^{cw}Nes-Cre^{+}* or *Tsc1^{cw}Nes-Cre^{++}* males or by breeding *Tsc1^{cw}Nes-Cre^{++}* females with *Tsc1^{cc}Nes-Cre^{-}* males. All *Tsc1^{cc}* animals were also homozygous for β-galactosidase from which β-gal expression is seen only after recombination. In the Tsc1 conditional allele exons 17 and 18 are floxed with loxP sites that are deleted at floxed sites in the presence of the Cre recombinase. As a result a *Tsc1* null allele is created according to time and area of Nestin promoter expression. Littermates with the genotypes *Tsc1^{cc}Nes-Cre^{-}* (cc^{-}) or *Tsc1^{cw}Nes-Cre^{-}* (cw^{-}) were used as control mice. To accomplish a mutant rate of 50% for the P0 studies *Tsc1^{cw}Nes-Cre^{+}* (*cw^{+}*) littermates were used as controls as we did not see any severe phenotype in the *Tsc1^{cw}Nes-Cre^{+}* animals later on in life.

Rapamycin powder was dissolved in 100% EtOH to obtain a stock of 20mg/ml and diluted in sterile vehicle directly before use (2.5ml 5% Tween, 2.5ml 5%PEG, 45ml dH_2O). Pregnant females were treated subcutaneously with one dose 1mg/kg rapamycin between embryonic day 11 and 17 in initial trials, later and for all P0 experiments on embryonic day 16. Postnatal treatment was started with 1mg/kg intra peritoneal on pups between day 7 and 9 after birth and then followed by the treatment schedule as shown in

figure 3 until the age of 21 days following by treatment every other day. In some studies mice were monitored every other day for body weight and survival. In other studies mice were sacrificed by decapitation between P0 and P2 or with CO_2 at older ages and were furthermore used for western blotting or histological analysis.

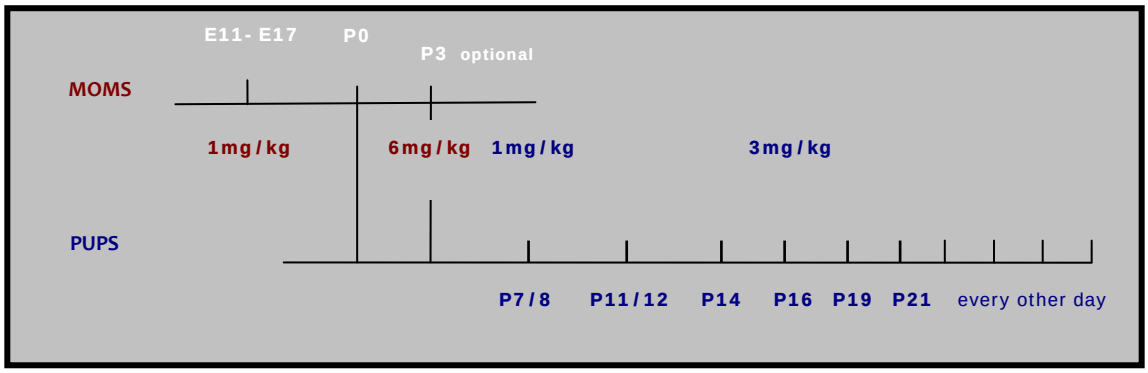

Figure 3: Rapamycin treatment schedule; injections on pregnant mice were given subcutcaneously, all other injections intra peritoneally

2.2.2 Rapamycin level measurements in tissue lysates

To investigate weather rapamycin can be transmitted from lactating mothers to pups, tissue lysates from pup brains as well as from liver, serum and brain from the mother were prepared. The mother was treated on P3 with a dose of 6mg/kg intraperitoneally of rapamycin. Mother and offspring were sacrificed 24 hours later and tissues were lysated in 1xPBS whereas 150 mg tissues were homogenized in 250 µl PBS. After homogenisation samples were centrifuged for 10 min at 4°C. Supernatant was further proceeded in Childrens Hospital Lab Control Core and Rapamycin levels were measured by mass spectrometry.

2.2.3 Blood tests

Blood was collected from newborns after decapitation. By using heparin coated capillaries blood clotting was avoided. Blood cell counting was performed on within 48 hours after collection in cooperation with Yoji Andrew Minamishima, MD, PhD (Dana-Farber Cancer Institute).

2.2.4 DNA isolation and analysis

For the regular genotyping DNA was isolated from mouse toes or tails by using a quick isolation protocol. 5-10 mg of the tissues were incubated with 100 µl TETT buffer (see 3.1.4) and 1 µl of proteinase K for over night at 65°C and were boiled for 15 min. For genotyping at the Tsc1 locus

a three-primer set was used to determine the conditional allele and the wild type allele simultaneously (figure 4). In addition a primer set that amplifies a 465 bp part of the Cre-recombinase gene was used to confirm the presence of the Nestin-Cre allele. Primer stocks were kept at a concentration of 200 µmol and were then diluted 1:10 in dH_2O for the working solution. For all PCR reactions in a PTC-100^{TM} Programmable Thermal Controller, 20 nM of each Primer was mixed with 0.8 µl of 25 mM dNTP, 2 µl of 10x Buffer and 0.15 µl of Ampli Taq Gold. The initial denaturation step of 9 min at 92°C was followed by 34 circles with a denaturation of 30 seconds at 92°C, an annealing of 30 seconds at 55°C and an elongation of 1 min at 72°C.

PCR products were mixed with 5 µl of 6x loading dye and loaded on a 2% agarose gel. After a running time of 10 min at 250 mV gels were investigated with Gel Doc 1000 (BioRad) imagining system and the software Quantity One.

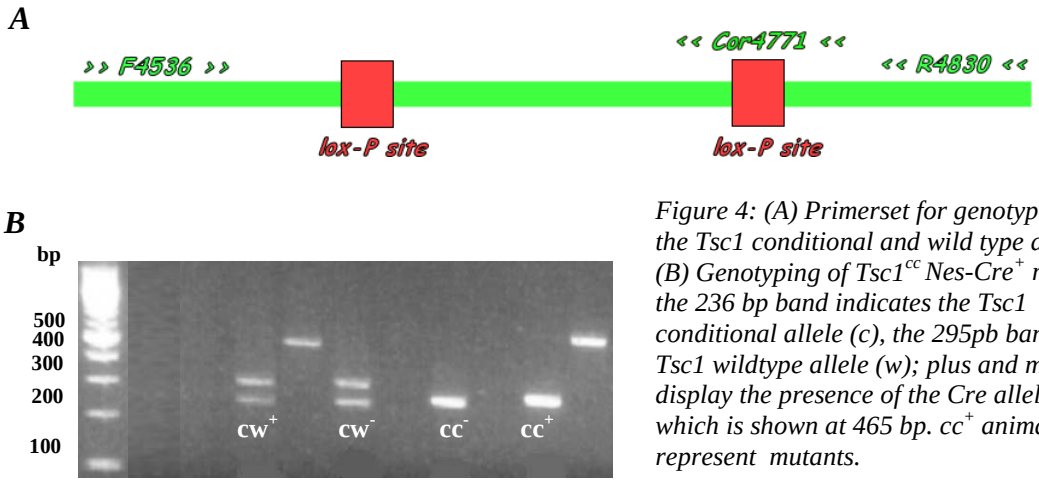

Figure 4: (A) Primerset for genotyping the Tsc1 conditional and wild type allele; (B) Genotyping of Tsc1^{cc} Nes-Cre^{+} mice; the 236 bp band indicates the Tsc1 conditional allele (c), the 295pb band the Tsc1 wildtype allele (w); plus and minus display the presence of the Cre allele which is shown at 465 bp. cc^{+} animals represent mutants.

For determining hetero- or homocygostity at the Cre-recombinase allele MLPA (Multiplex ligation-dependent probe assay) analysis was done as previously described (Kozlowski et al., 2007). For that purpose a different DNA isolation protocol was required. Toe snips were incubated with 150 µl of cell lysis solution and 1.5 µl (20 mg/ml) Proteinase K for 3 hours to overnight at 65°C. The lysates were incubated with 1.5 µl (4 mg/ml) RNAse A for 20 min at 37°C. After adding 100 µl of protein precipitation solution and an incubation of 5 min on ice, samples were centrifuged for 3 min at 15000rpm. The supernatant was well mixed with isopropanol by inverting min. 50 times followed by 5 min centrifugation at 16000rpm. The isopropanol was removed and replaced by 300 µl 70% Ethanol and centrifuged for 1 min

16000rpm. After air drying the DNA was resolved in 100 µl hydration solution. For MLPA analysis DNA concentration was measured by spectrophotometer and equal amounts of DNA (50 ng/µl) were analyzed in the DNA Sequencing Core.

2.2.4.1 MLPA analysis

MLPA analysis was performed by a chief technician at DNA sequenceing core Mei-Huang Lin as described previously (KOZLOWSKI et al., 2007). For the Nestin-Cre transgene two MLPA probe sets were designed to have amplification products of size approximately 120 bp and 170 bp. In addition three control probes elsewhere in the mouse genome were used ranging in size from 108 10 136 bp. During MLPA, an oligonucleotide ligation reaction was performed, followed by PCR using a fluorescence-conjugated primer, so that the amount of PCR product is directly proportional to the number of copies of the target sequence. The amount of copy number is represented by the peak heights in the electropherogram.

2.2.5 Histology and Immunohistochemistry

2.2.5.1 Paraffin-embedded sections and Immunohistochemistry

For regular histological analysis treated and untreated mice were sacrificed in carbon dioxide or pups at P0 were decapitated and the whole body was fixed in bouin's solution (Sigma). Paraffin sections in a thickness of 5 µm, H&E and Nissl stainings were done in the DF/HCC Research Pathology Core for Rodent Histology.

For immunohistochemical staining with pS6 and PCNA, sections were deparaffinized and hydrated with xylenes and graded ethylalcohol series ending with distilled water. The antigen retrieval was performed in boiling citrated buffer. Slides were placed for 20 minutes in boiling or just below boiling 10 mM citrate buffer (pH 6, Dako). After cooling down for 20-30 minutes slides were washed in water (3×2 min) and endogenous peroxidase activity was quenched by incubating the slides in 1% Hydrogen Peroxide for 30 minutes. Washing in TBST (3×5 min) was followed by the blocking step in blocking solution (1×TBS with 2% normal serum, 1% BSA) for 20 minutes. Primary antibodies were diluted in blocking solution in the desired concentration an incubated at 4°C for over night followed by washing in TBST (3×5min). The Horseradish Peroxidase (HRP) - labeled secondary antibody against rabbit was used as described in the Dako Envision Kit. After three washing steps in TBST the DAB substrate was diluted in the adequate buffer as described by the manufacturer. Slides were incubated in DAB solution until staining is

optimal and counterstained with hematoxylin. After cleaning in graded ethyl alcohols and xylenes the slides were mounted with xylene based mounting medium.

2.2.5.2 Frozen sections and Stainings

For frozen sections embryos and tissues were dissected and fixed in 1% Paraformaldehyde (PFA) for overnight at 4°C. After dehydration in 30% sucrose around 24h, the samples were embedded in Tissue Freezing Medium (obtained from Triangle Biomedical Sciences, Inc.) and sectioned on a cryostat in a thickness of 20 µm.

For **5-Bromo-4-chloro-3-indolyl-β-D-galactopyranoside (β-Gal) staining** to assess β-gal expression samples were air dried and postfixed in 0.2% PFA at 4°C for 10 min followed by two washing steps (PBS with 2 mM $MgCl_2$) 10 min each. After 10 min incubation in detergent rinse at 4°C the samples were left in lacZ staining solution for over night at 37°C. After two washing steps the samples were counterstained with Nuclear Fast Red, dehydrated in descending methylalcohol steps ending with xylene and mounted in Vecta Mount.

2.2.6 Immunoblotting / Western Blot Analysis

Mice were sacrificed at P0 and P21 respectively and either whole brain from newborns or cortex from older animals was dissected, lysated in PBS and centrifuged 10 minutes at 4°C. The concentration of the lysates was measured by spectrophotometer and equal amounts of protein extract (20-80 ng) were separated by SDS-PAGE and transferred to a PVDF membrane. Membranes were further treated following the stripped technique in which membranes are cut an incubated with the primary antibodies according to the molecular weight of their target protein. After blocking the membrane in blocking solution primary antibodies for different proteins (antibodies and dilutions listed in 3.1.7) were applied to the membrane pieces and incubated for over night at 4°C. After washing the secondary antibody was incubated for 30 min at room temperature and that step was followed by another washing step. For envision the SuperSignal®West Pico and Femto, respectively, was used and analysis were done after developing film or with Syngene (G:BOX) envision system.

2.2.7 Cell size Measurements

Pictures for cell size measurement were taken in a magnification of 40x from Nissl stainings. Motor cortex of the anterior hippocampus was defined according to the “Atlas of the Developing

Mouse Brain" (Paxinos et al., 2007) and 2 pictures of the motor cortex were taken per animal. In each picture the five largest cells were measured by ImageJ software and transcribed to Prism4.

2.2.8 Statistics

Statistic evaluations were performed with Prism4 software. P-values were calculated by using nonparametric t-test with a confidence interval of 0.95 and are indicated by stars (* $p< 0.05$, ** $p< 0.01$, *** $p< 0.005$).

3 RESULTS

3.1 Mouse breeding & MLPA analysis to get *Nes-Cre*$^{++}$ parents, which accelerates the breeding for getting *Nes-Cre*$^{+}$ mutants

In order to accelerate the breeding to obtain *Tsc1*^{cc} *Nes-Cre*$^{+}$ mutants in higher incidence we crossed our *Tsc1cc* to *Tsc1*^{cw} *Nes-Cre*$^{++}$, in which we expect mutants in 50% of offspring. MLPA was performed to analyze the zygostiy status of Nestin-Cre recombinase allele of pups. Analysis of the data from MLPA was done in Exel®. Normalization of the peak height data was done by normalizing the transgene peak height to the average heights of the three control probes. As a result two groups were seen in the scatterblot graph, the upper cluster represents for Nes-Cre homozygous animals, the lower for heterozygous animals (figure 5).

A

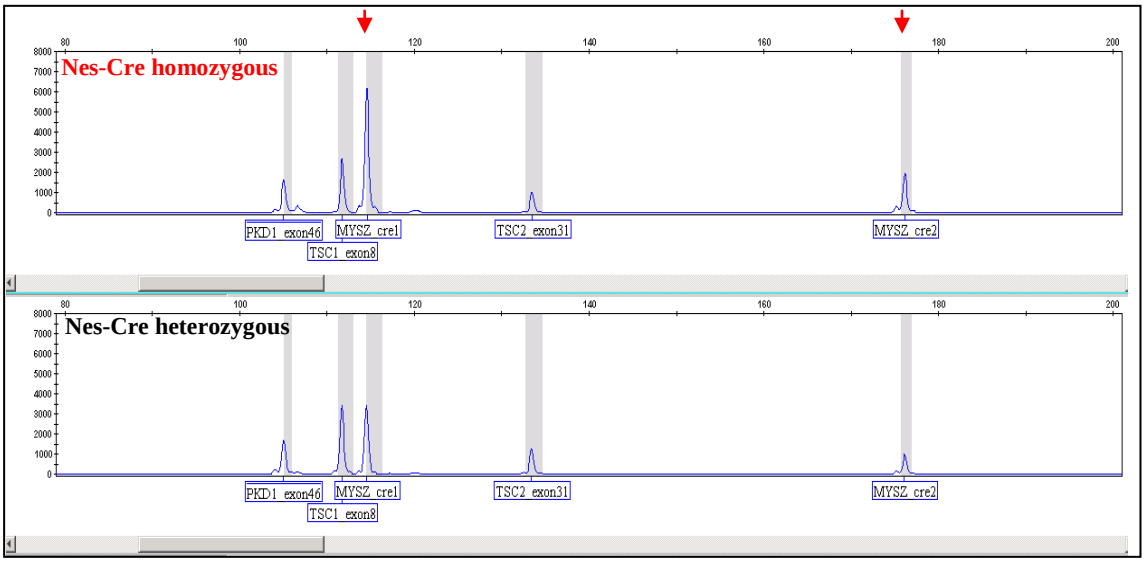

B

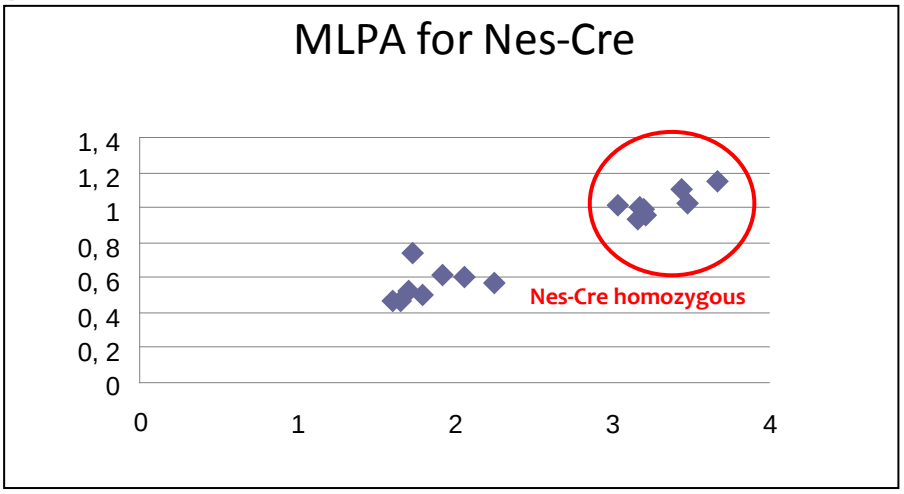

Figure 5: (A) Electropherogram of a homozygous and a heterozygous mouse for Nes-Cre; (B) Diagram of normalized peak heights from 2 sets of Nes-Cre probes in MLPA analysis.

3.2 Organs and tissues in which Tsc1 recombination occurs in *Nes-Cre*$^{+}$ mice

3.2.1 Embryonic day E16.5-17.5

The expression pattern of Cre-recombinase in *Nes-Cre*$^{+}$ mice was confirmed by β-Galactosidase (β-Gal) staining. As expected, major recombination occurred in the central nervous system (figure 6A) and in dorsal root ganglia (6B) as well as in the developing kidneys (6E) and eyes (D). Some isolated blue cells were seen in cartilage, heart, lung and connective tissues in the skin.

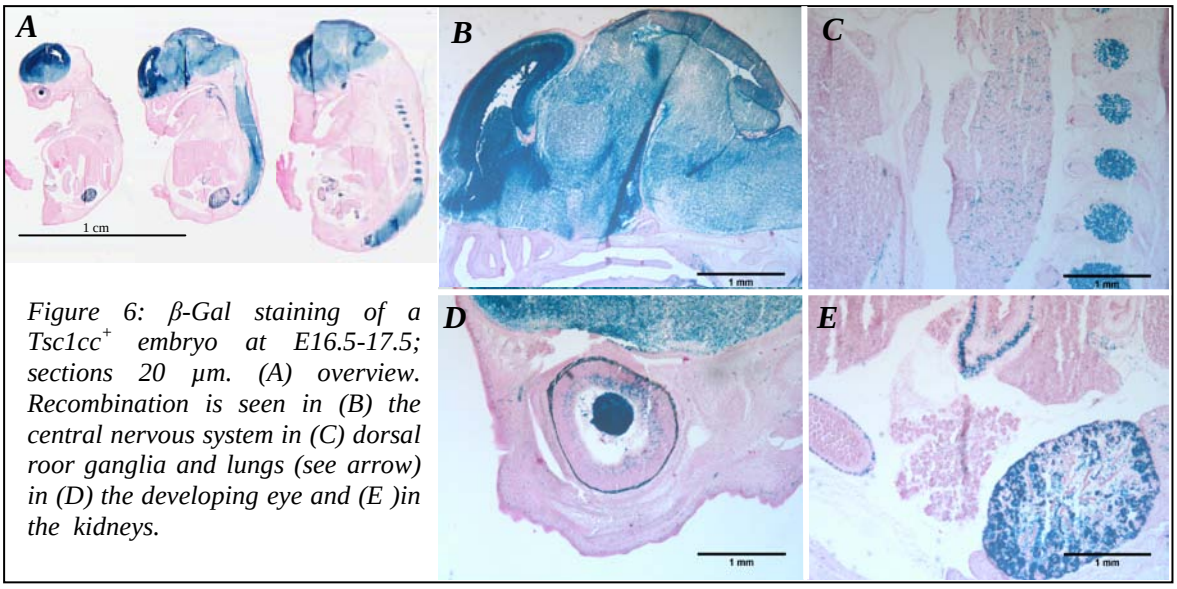

Figure 6: β-Gal staining of a Tsc1cc^{+} *embryo at E16.5-17.5; sections 20 µm. (A) overview. Recombination is seen in (B) the central nervous system in (C) dorsal roor ganglia and lungs (see arrow) in (D) the developing eye and (E)in the kidneys.*

3.2.2 Postnatal Day 2

Similar recombination pattern was seen at the age of two days in *Nes-Cre*$^{+}$ mice (figure 7).

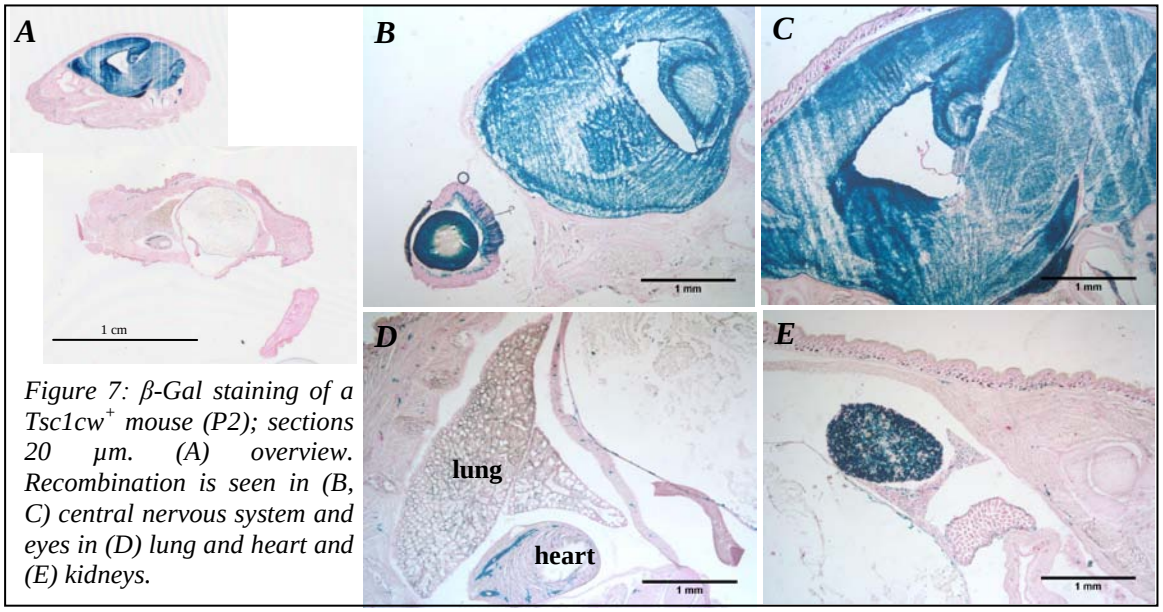

Figure 7: β-Gal staining of a Tsc1cw^{+} *mouse (P2); sections 20 µm. (A) overview. Recombination is seen in (B, C) central nervous system and eyes in (D) lung and heart and (E) kidneys.*

3.3 Pre- and postnatal Rapamycin Treatment

3.3.1 Survival

Tsc1^{cc} *Nes-Cre*$^{+}$ pups were born in Medelian ratio, but all of them died short after birth within 24 hours (figure 8A, green). To determine the potential benefit of rapamycin in embryos, pregnant mothers bearing controls and *Tsc1*^{cc} *Nes-Cre*$^{+}$ pups, were treated prenatally between E11 and E18 and pups consequently postnatally (2.2.1). The time range of prenatal treatment was chosen in a wide range, because the optimal time point in embryonic development was not known. P0 experiments with E16 treatment were done based on the results that show that best survival was obtained after prenatal treatment between E15 and E17.

With only one prenatal dose or one prenatal and one postnatal dose on lactating moms (figure 8A, blue cohort) the survival was already increased to a median survival of 13 days. It must be mentioned that in this cohort the death of mutant mice at birth was not monitored, but it is very likely that a part of the mutant mice still die at P0, dependent on litter size, their possible disadvantage in strength compared to their control litter mates and on the behavior, age and care of the mother. This observation was made in the cohort of pre- and postnatal animals. Also a natural death rate occurs among control animals due to same reasons. With prenatal treatment on pregnant moms and postnatal treatment on the pups themselves the median survival was increased to 20 days on average (figure 8A, red cohort).

Because the optimal time point of prenatal rapamyin was not known we treated pregnant mother between embryonic day 11 and 18. Due to these initial studied it is suggested that early and late treatment during gestation had an adverse effect on the offspring survival. Best results were accomplished by treating pregnant moms between embryonic day 15 and 17 (figure 8B). Therefore E16 we suggest that E16 is the optimal time point of prenatal rapamycin treatment with best therapeutic effects. This outcome was used to arrange experiments on newborn animals.

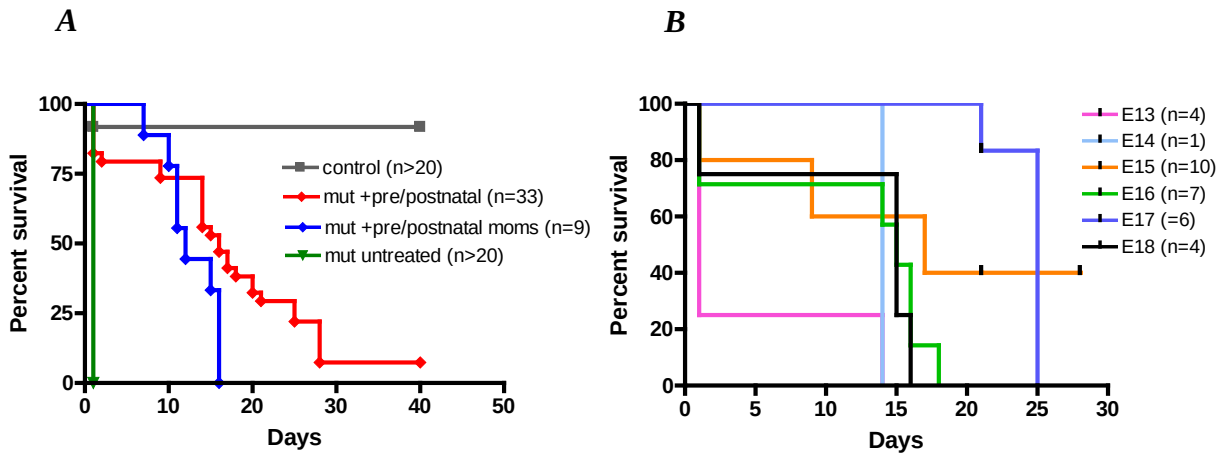

Figure 8: (A) survival of Nes-Cre^{+} animals without treatment (green), with prenatal treatment and/or postnatal treatment on moms (blue) and with prenatal treatment on moms and postnatal treatment on pups (red). Prenatal treatment time points reached from E13 to E18. Some animals were monitored without intervention; some were sacrificed for further investigation and were considered as "survived" in the graph. Animals that were sacrificed due to weakness and overall bad condition were considered as "died". (B) red cohort from figure 8A is splitted up showing survival dependent on the prenatal time point of rapamycin injection.

3.3.2 Efficiency of postnatal treatment on lactating mothers

We hypothesized that rapamycin could be transmitted through the milk, and have effects to the pups brain. To investigate if and how much rapamycin can be transmitted such that administration to nursing mothers would lead to appreciable dosage in the pups. Levels of rapamycin were measured in brain, liver and serum of the mother and in the brain of the offspring 24 hours after a dose of 6 mg/kg i.p. at P3. Brain levels of rapamycin ranged between 3 and 7 ng/g in the pups. Therapeutic levels in patients are described as 3-20 ng/ml blood (MEIKLE et al, 2008). Even though the brain levels of rapamycin in the pups were within the therapeutic range, no benefit could be seen in the survival of pups with an additional postnatal treatment on lactating moms between 3 and 7 days after birth (figure 9B). Therefore, to prevent mice from another injection as a stressful event, this additional treatment was omitted in further experiments.

A

ID	*ng/ml*	*ng/g*
Pup 1	1.6	3.9
Pup 2	2.6	6.76
Pup 3	1.4	3.72
Pup 4	1.6	4.13
M liver	50.8	126.4
M serum	104.2	-
M brain	11.3	27

B

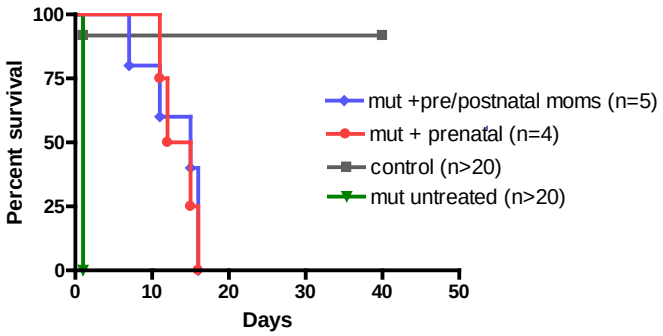

Figure 9: Rapamycin measurement in brain tissue of pups 24 hours after the treatment on the lactating mother. (A) Levels of rapamycin in brain tissue of 4 pups and liver, serum and brain of the mother, (B) survival f pups dependent on the treatment of the mother

3.4 Characterization of the mouse model and effects of Rapamycin in newborn mutant mice

All the following experiments connected to investigations on the primary characterization of the *Tsc1*^{cc} *Nes-Cre*$^{+}$ mouse model were performed on newborn mice, due to the perinatal death of untreated mutant animals. All results in this paragraph (3.4.) show data from P0 pups. Treated animals were generated by prenatal subcutaneous injection of 1 mg/kg rapamycin to the pregnant mother on embryonic day 16 (E16) and the pups were sacrificed perinatally. Usually in adult brains the distance from the bregma (area of skull where the frontal bone and the parietal bone come together) is used to define every location in coronal planes of the brain. Because the brain of newborn mice is still in development and therefore much different in size and morphology all specifications about the brain area are shown as described in the “Atlas of the Developing Mouse Brain” (Paxinos et al., 2007). Planes of coronal sections are shown by numbers in millimeter indicating the distance from the most rostral section in the series (e.g. the number 3.87 above the scale in figure 10 means that the shown plane is 3.87 mm far from the very rostral beginning of the brain).

Although mutant mice die short after birth they were undistinguishable in body weight and appearance at P0. In addition, all offspring show milk in the gut independent on their genotype.

3.4.1 Increased Brain/Body Weight Ratio

Tsc1^{cc} *Nes-Cre*$^{+}$ mice at P0 showed bigger brains (figure 10A and B) and an increased brain weight compared to the control (*cw*$^{+}$) littermates (figure 10C). The body weight of the mutant mice was only mildly lower which resulted in a significant higher brain to body ratio in mutants (figure 10C).

Rapamycin treatment at E16 did not influence brain size and weight but did have a significant impact on body weight in all genotypes tested. 18.4% body weight reduction was seen in control and 18% in mutant mice, suggesting one of the possible side effects of rapamycin treatment (figure 10C).

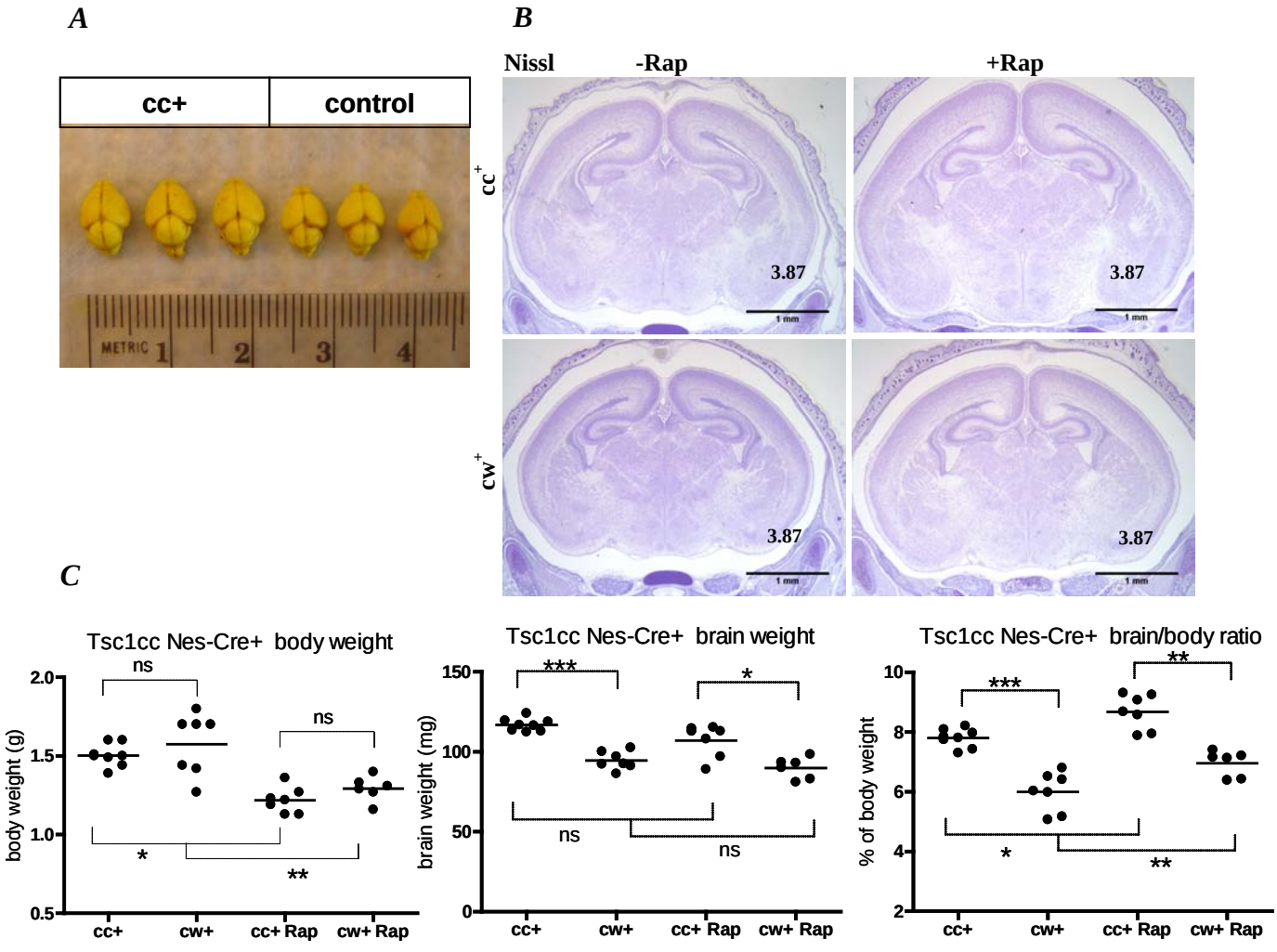

Figure 10: brain and body data of P0 pups: (A) macroscopic comparison of brain size of Nes-Cre^{+} *mice to control animals showing bigger brains in mutants (provided by Kristen Pollizzi and June Goto, PhD). (B) coronal brain sections with (+Rap) or without (-Rap) prenatal rapamycin treatment indicating that one dose of prenatal rapamycin has no effect on brain size [n=2 (cc*$^{+}$*), n=3 (cw*$^{+}$*), n=3 (cc*$^{+}$*/+Rap), n=2 (cw*$^{+}$*/+Rap). (C) body weight, brain weight and brain to body ratio [n=8 (cc*$^{+}$*), n=7 (cw*$^{+}$*), n=7 (cc*$^{+}$*/+Rap), n=6 (cw*$^{+}$*/+Rap)]*

3.4.2 Disorganized Layer formation and enlarged neurons in the motor cortex

Although in newborn mice the six cortical layers are not clearly developed because of ongoing migration, in all *Tsc1*^{cc} *Nes-Cre*$^{+}$ mice tested the layer arrangement was less distinct than in control mice (figure 11B). Cells were spread out throughout the cortex which may be one of the

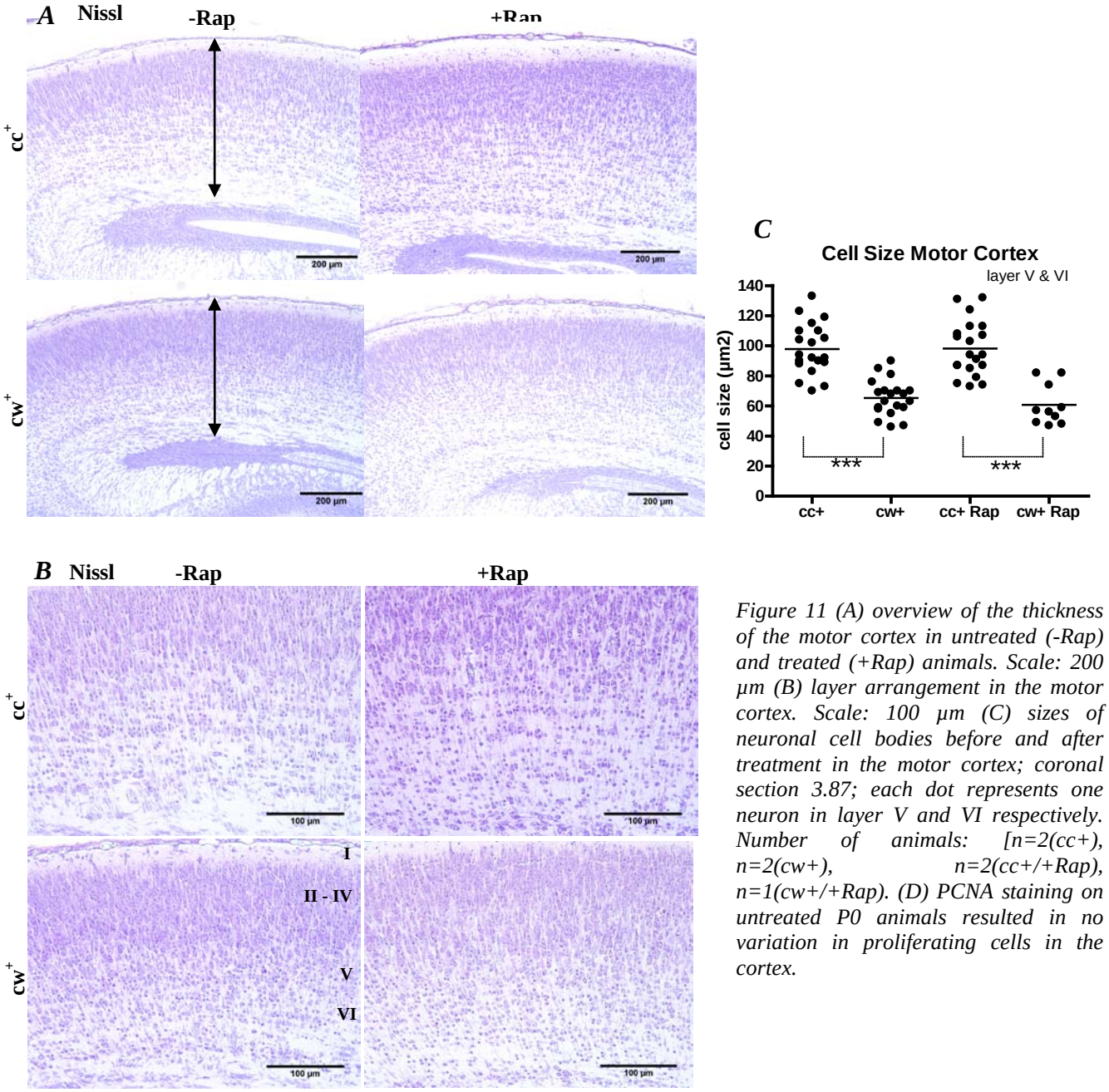

Figure 11 (A) overview of the thickness of the motor cortex in untreated (-Rap) and treated (+Rap) animals. Scale: 200 µm (B) layer arrangement in the motor cortex. Scale: 100 µm (C) sizes of neuronal cell bodies before and after treatment in the motor cortex; coronal section 3.87; each dot represents one neuron in layer V and VI respectively. Number of animals: [n=2(cc+), n=2(cw+), n=2(cc+/+Rap), n=1(cw+/+Rap). (D) PCNA staining on untreated P0 animals resulted in no variation in proliferating cells in the cortex.

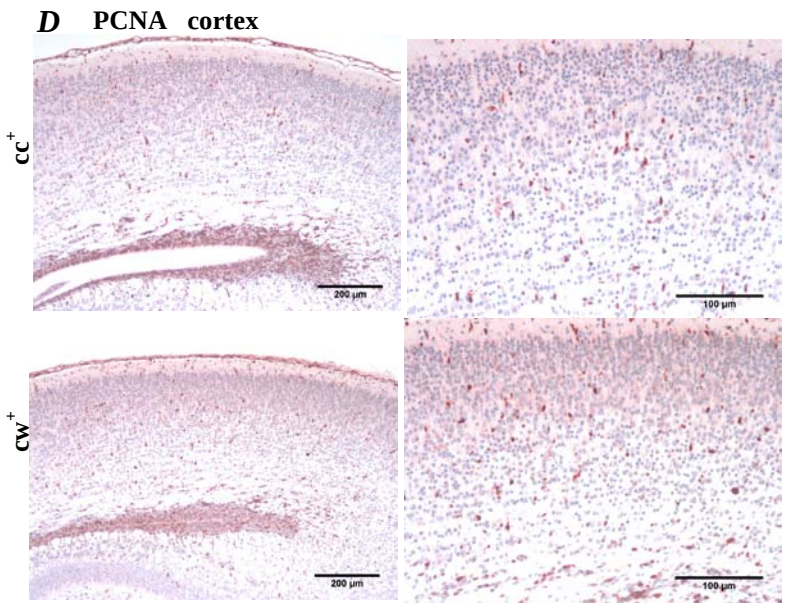

reasons for the observed increase in brain size. However, the density of cells seems not to be higher. The thickness of the cortex was around 17 % increased in mutants in average and the rapamycin treated group did not show any reduction. (figure 10B, figure 11A). The sizes of neuronal cell bodies in layer V and VI of the motor cortex were measures as described in 3.2.6. and were 34.7% bigger in *Tsc1*^{cc} *Nes-Cre*$^{+}$ mice than in control animals before treatment and 37.8% bigger after treatment (figure 11C). Furthermore, paraffin sections were stained with PCNA (Proliferation Cell Nuclear Antigen) which is a marker for proliferating cells (PAUNESKU et al., 2001). The cortex of *Tsc1*^{cc} *Nes-Cre*$^{+}$ mice showed no differences in PCNA staining in all genotypes tested, suggesting no changes in cell proliferation in the cortex of mutant mice elevation of proliferating cells (figure 12).

3.4.3 Hippocampus formation

Looking at the overall brain histology subtle disorganization of layers could be seen in the dentate gyrus of the hippocampus of *Tsc1*^{cc} *Nes-Cre*$^{+}$ formation compared to wildtype mice as shown in figure 12. The hippocampus is known to be the only site in the brain in which proliferation occurs beyond P0 and in older ages. Therefore, proliferation was investigated with performing PCNA staining on paraffin section as described before. As observed in the cortex no differences of proliferation was observed in the hippocampus formation in cc+ mutant mice compared to wildtype mice.

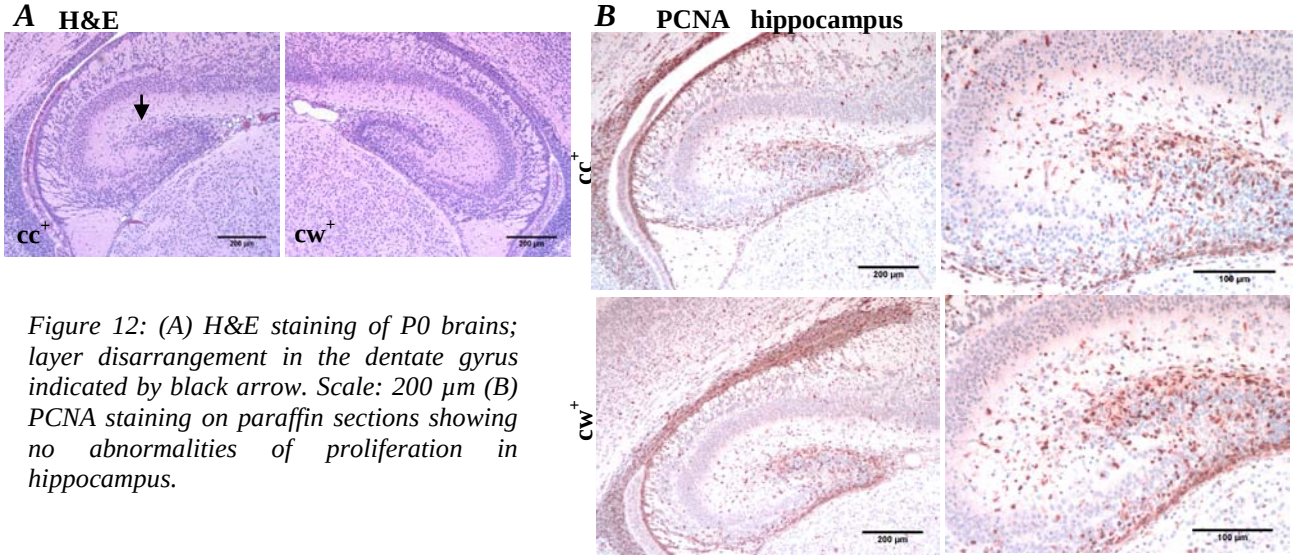

Figure 12: (A) H&E staining of P0 brains; layer disarrangement in the dentate gyrus indicated by black arrow. Scale: 200 µm (B) PCNA staining on paraffin sections showing no abnormalities of proliferation in hippocampus.

3.4.4 Western Blot and IHC for protein analysis

Western blot analysis of P0 brain lysates was performed to monitor the expression of a number of relevant proteins (figure 13). Western blot of P0 *cc*$^{+}$ pups compared to *cw*$^{+}$ shows lack of Tsc1 and a lower level of Tsc2 protein expression in brain tissue (figure 13A). Since it has been reported that Tsc2 protein is stabilized by Tsc1 in the functioning protein complex, as expected also Tsc2 is degraded in Tsc1 null animals and protein levels were clearly reduced. Looking at the untreated mice group (figure 13A, left panel) phosphorylation of pS6 in the mutants was increased at both phosphorylation sites (pS6 Ser240 and Ser235) compared to wildtype mice indicating the higher activation of mTOR due to Tsc1 loss (KWIATKOWSKI 2003). Increased phosphorylation of pS6 due to mTOR activation induces a negative feedback loop in which S6K

initiates the degradation of IRS and less activation of AKT through PI3K (MEIKLE et al., 2008). This explains why the levels of phospho-AKT were lower in the mutants compared to wildtype controls as expected. In contrast, rapamycin treated mutant animals (right panel) showed a lower pS6 level, especially pS6 (235), indicating that one prenatal dose of rapamycin given at E16 is probably sufficient to decrease mTOR activity. Surprisingly, rapamycin treatment did not influence phosphorylation of AKT in mutants. Control animals showed lower pS6 levels after treatment but surprisingly also lower activation of pAKT (figure 13A). Results of immunoblotting were confirmed by using another set of litters for treated and untreated mutant and control pups at P0.

Higher levels of phosphorylated S6 protein were additionally confirmed by immunohistochemistry on paraffin sections of the motor cortex (figure 13B). Highly positive and ectopic neurons were detected in the mutant mice which tend to be bigger than lightly stained or unstained cells (arrows). Rapamycin treatment depleted the frequency of ectopic, positive cell and also caused a reduction of pS6 levels in control animals (figure 11B).

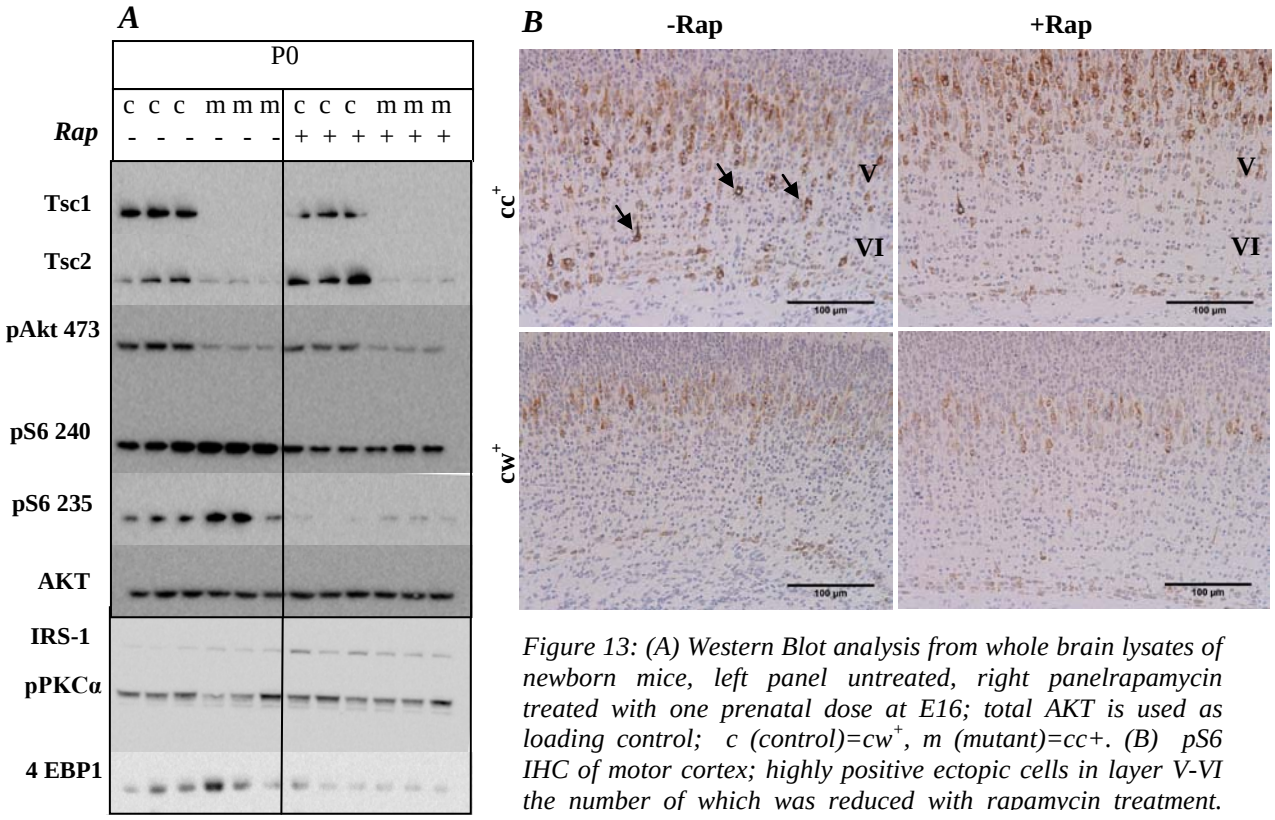

Figure 13: (A) Western Blot analysis from whole brain lysates of newborn mice, left panel untreated, right panelrapamycin treated with one prenatal dose at E16; total AKT is used as loading control; c (control)=cw+, m (mutant)=cc+. (B) pS6 IHC of motor cortex; highly positive ectopic cells in layer V-VI the number of which was reduced with rapamycin treatment.

3.5 Further investigations on newborn untreated *Tsc1 cc Nes-Cre+* mice

As shown before the recombination in *Tsc1*^{cc} *Nes-Cre*$^{+}$ mice occurred at high level in the whole brain but interestingly when looking at the cortex only a few cells seemed to be affected by high mTOR activation as seen in the pS6 staining (figure 13B). First, it is possible that other areas of the brain not yet analyzed could be affected in some way and cause dysfunction. Second, other sites of the body may show abnormalities as we observed β-Gal staining in additional organs (figure 6, figure 7). Immunohistochemistry for pS6 showed similar levels of pS6 in hippocampus, cerebellum and brainstem of mutant and wildtype mice (data not shown). Some nuclei in the thalamus seemed to have higher expression of pS6 which is discussed in section 6. Still investigations are ongoing to determine if other affected areas in the brain could contribute to the early death. Although, looking at the gross brain and body pathology of untreated newborn mutants, no obvious striking lesions were visible. Basic life supporting functions like first breathing and nutrition uptake were not affected, as no correlation between milk in the gut and mouse genotype has been seen in the pups.

3.5.1 Kidney

As showed in the β-Gal staining in section 4.2. the central nervous system is not the only tissue in which recombination occurs. Therefore other tissues in newborn mutants were analyzed. The only location in which small lesions were clearly seen in histological sections stained with H&E was the kidney. Dilated tubules in the medulla of the kidney were found as shown in figure 14. However, it seemed to be unlikely that such mild lesions may lead to lethality, as the surrounding tissue appeared histologically normal and usually kidneys can compensate moderate lesions (Zhou et al., 2009). Interestingly, after rapamycin treatment given prenatal the observed dilated tubules could be extincted (figure 14, right panel).

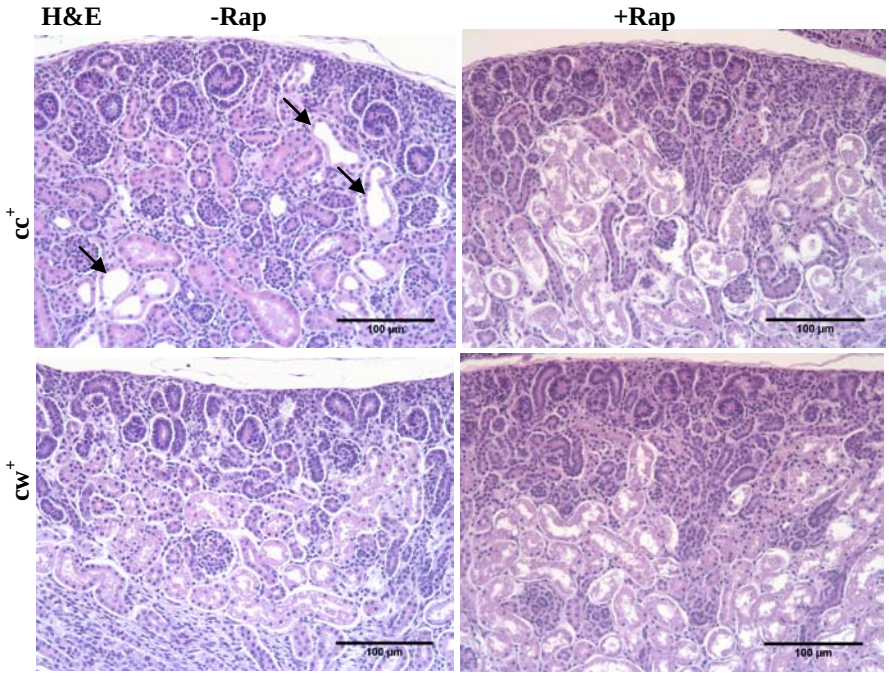

Figure 14: H&E staining of kidneys from newborn mice. rapamycin treatment could reverse the occurrence of dilated tubules seen in untreated animals. scale: 100µm

3.5.2 Blood

Preliminary blood tests were performed on one E16 treated litter and one untreated litter at P0. Blood glucose levels were measured from the latter as well. As seen in figure 15 significant differences in hemoglobin (Hb) and hematokrit (HTC) were seen in untreated pups. Mutants tended to have a higher amount of Hb and increased HTC whereas the total number of red blood cells (RBC) was unchanged which may indicate an increase in red blood cell size. Blood count of total white blood cells, neutrophils, monocytes and platelets resulted in non-significant differences between cc^+ and cw^+ animals. In contrast, blood glucose levels tended to be lower than the normal expected value in P0 mice that is between (50-70 mg/dL) which was also described previously (in a murine model of neonatal diabetes mellitus) (WATANABE et al. 2009). Still, this set of data is preliminary due to the small number of animals tested.

Rapamycin treatment results in an increase of white blood cells (WBC), RBC, Hb and neutrophils but a decline in HCT.

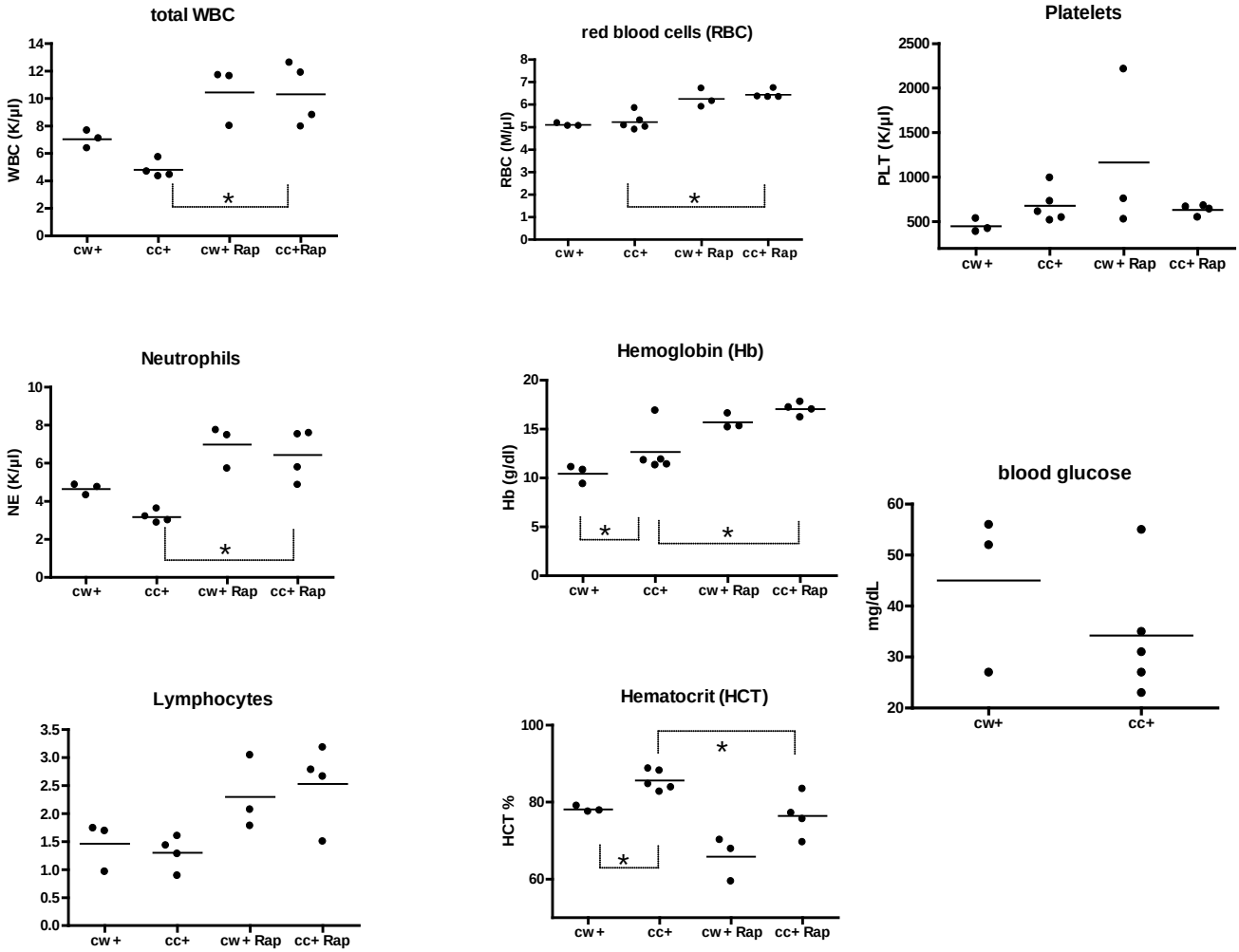

Figure 15: Blood cell counting results and glucose levels of an untreated litter and a litter with prenatal rapamycin treatment at E16. p-values ($p<0.05$) are only marked in graphs in which significant differences between two groups are seen.

3.6 Phenotypic characterization of treated *Nes-Cre*$^{+}$ mice

Although rapamycin treatment caused a significantly increased survival, mutant mice still show a clear phenotype. Most obvious was the severe underweight and the lack of weight gain during further development that was seen in all of the mutant animals. As shown in figure 16 *cc*$^{+}$ animals hardly reached more than 5 grams until the age of 20 days, whereas control animals weighed roughly twice as much at the same age (figure 17). Most of them also displayed tremor, straub tail and delayed eye opening, some of them were incapable to turn around when placed upside down especially in younger mice (Table 1).

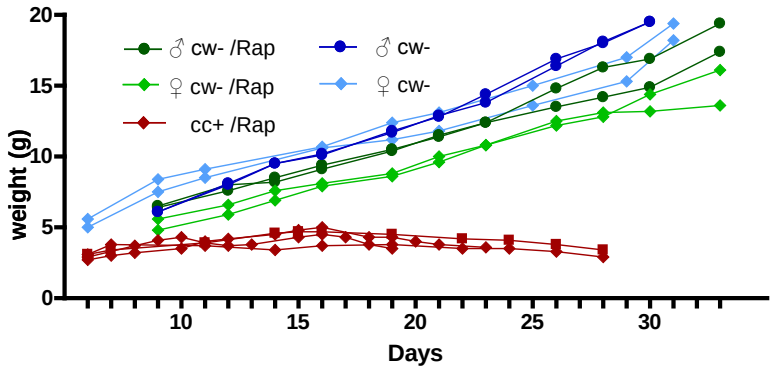

Figure 16: weight gain in postnatal development. Treated mutants and controls compared to untreated controls. Control animals were treated prenatal with a dose of 1mg/kg to the pregnant mother, postnatal treatment was performed using the treatment schedule (Figure 3) that was followed by application of 3 mg/kg rapamycin intraperitoneally every other day until P58. [n=4 (cw^{-}*/Rap), n=4 (cw*$^{)}$*, n= 33 ≥P2 (cc*$^{+)}$*)]*

Table 1: list of 8 treated mutant mice and monitored phenotypes; blank boxes indicate that data was not determined. Position of tail, tremor and sensitivity (jumpy) were scored in a 0-3 scale; colors indicate multiple data points for one individual animal; grade of eye opening was determined by using a scale from moderate (+) to completely closed (++); repetitive movements in circle are indicateted by direction of movement left (l) or right (r).

ID	*age (d)*	*weight (g)*	*tail*	*tremor*	*eyes*	*jumpy*	*circle*	*Inability to turn*
740	11	3		2				+
771	17	4,3	3		+	3		
784	19	4,3	3		+			
803	16	4,9			++			
	19	4,1			++			
	21	4,4	1	1	++			
	56	10,6		1			r	
808	11	3,7	2	2				+
	19	3,8	2	2	++			
	24	3,5			++			
	28	2,9		2	++			
809	11	3,9	2	2				+
	19	4,5	2	2	++			
	24	4,1			++			
	28	3,4		2	++			
1013	8	3,6					r	+
	14	3	2	2				
1030	16	3,9	2	1			l	

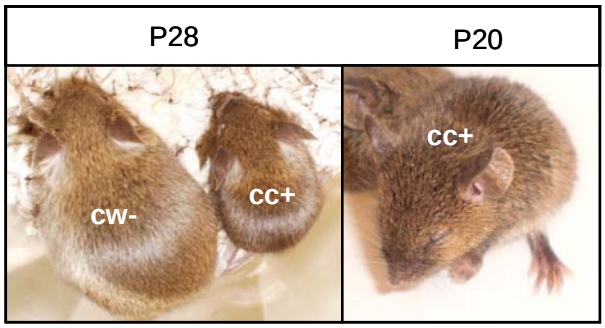

Figure 17: left: control mouse (cw^+) and treated mutant mouse (cc^+) at the age of 28 day with an obvious reduction in body weight seen in the cc^+ animal. Right: treated mutant mouse at P20 showing delayed eye opening

3.6.1 Protein expression levels at the age of P21 and P28

Analysis of protein expression by western blotting was performed for 3 mutant animals that were sacrificed at P21 and one animal at P28. The latter was sacrificed because of bad condition. As expected, Tsc1 protein in cc^+ animals is lacking due to recombination. Since Tsc2 is stabilized by Tsc1 in the functioning protein complex, also Tsc2 is degraded in Tsc1 null brains and protein levels are clearly reduced. Total AKT was used as loading control. Rapamycin treatment caused a significantly higher survival rate, which can be due to a compensation of the up regulated mTOR pathway (figure 18). As seen in the western blot, the pS6 levels were decreased in the mutants or even completely missing, looking at two different phosphorylation sites pS6 Ser235 and pS6 Ser240. Due to low S6K activation the negative feedback to AKT does not occur and the pAKT levels therefore elevated in the treated mutant mice. Furthermore GFAP (glial fibrillary acidic protein) which is widely used as a marker for astrocytes and astrocyte derived pathologies like glioblastomas, was increased, indicating enhanced proliferation of glial cells. In contrast the MBP (myelin based protein) was slightly decreased in P21 treated mutants but not in the P28

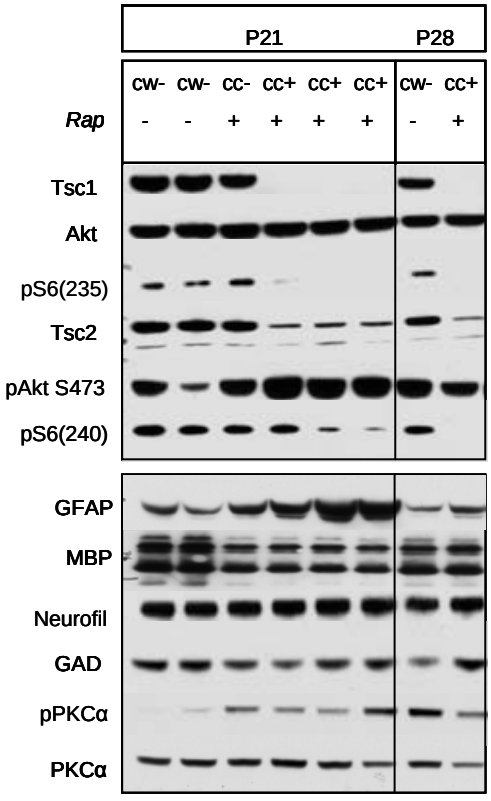

Figure 18: Western Blot analysis from P21 controls and mutatns as well as from 2 animals at P28. Lysates were prepared from cortex. Brains were dissected 2 days after the last rapamycin treatment. Immunoblotting has not been repeated on a greater number of animals.

mutant. No differences were seen in the levels of GAD (Glutamic Acid Decarboxylase) demonstrating no changes in the function of inhibitory neurons. Also PKCα expression levels were analyzed which is a downstream effector of mTORC2. Whereas absolute amounts of PKCα were similar in all animals, activated and phosphorylated PKCα is variable among mutants and controls and did not allow clear interpretation

3.6.2 Histopathology of treated *Nes-Cre*$^{+}$ mice at the age of 21 and 28 days

Material for brain pathology was unfortunately really restricted. Histology and Imunnohistochemistry of three mutant and control animals at P21 was planned but brain tissues got damaged during processing and could not be used for further investigation. More animals could not be generated again so far. Nevertheless in a preliminary analysis one untreated control and one treated mutant were sacrificed at P28 and histological sections were done (figure 19). Although it is not recommended to compare different planes of brain sections and mice of different ages, again enlargement of the cortex as well as mild hippocampus disorganization was clearly visible (figure 19).

GFAP and pS6 staining of P28 animals reflected the results seen in the western blot analysis. Even though the GFAP staining was faint, astrocytes were spread throughout the cortex in the mutant which is a sign of astrogliosis. pS6 staining was completely negative in the mutant mouse with rapamycin treatment. Obvious down regulation seen in the staining is again a hint that an overdose was administered (figure 20).

Kidneys displayed small cysts arranged in the cortico-medullary boundary but look normal apart from that. Major dysfunction was not being expected from those lesions. In contrast the bone marrow displayed a lack of blood progenitor cells and an infiltration of red blood cells which is a sign of aplastic anemia. A side effect of rapamycin could be excluded as treated control showed normal bone marrow (figure 21).

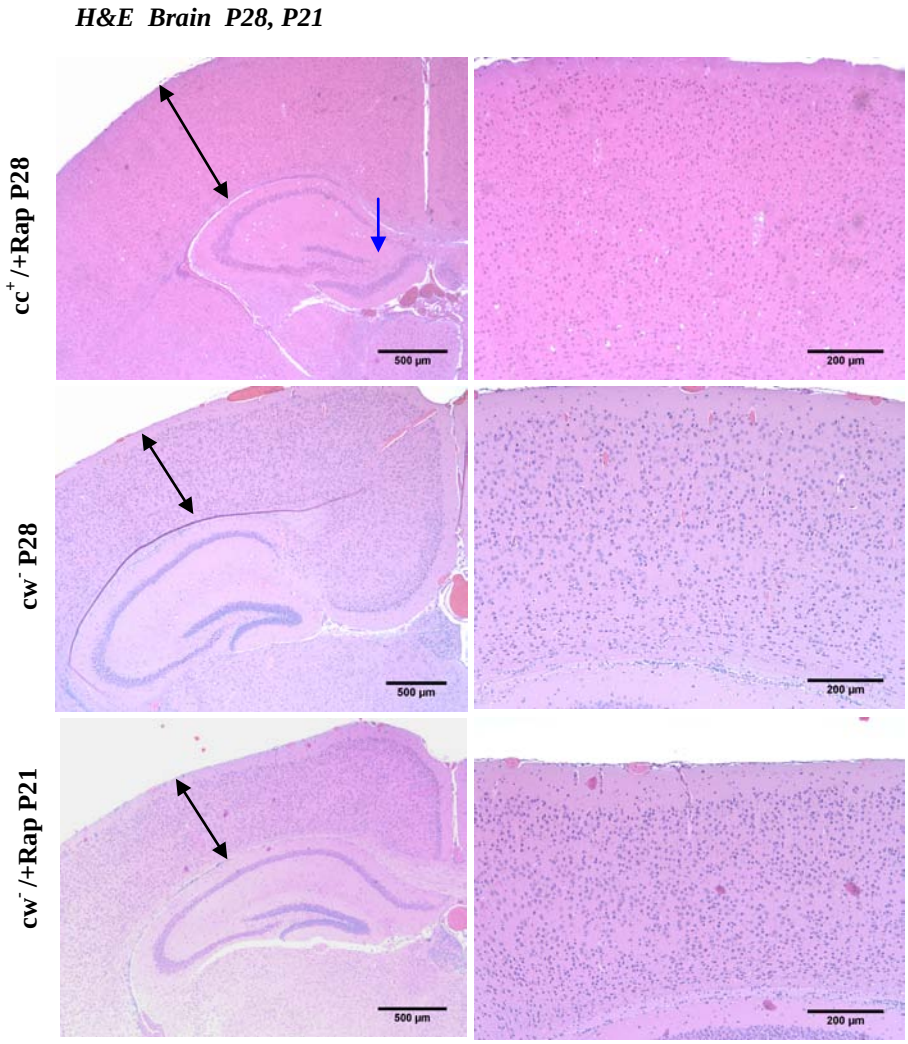

Figure 19: H&E staining of P28 and P21 brains. Thickness of the cortex indicated by black arrows, and hippocampus disorganization indicated by the blue arrow.

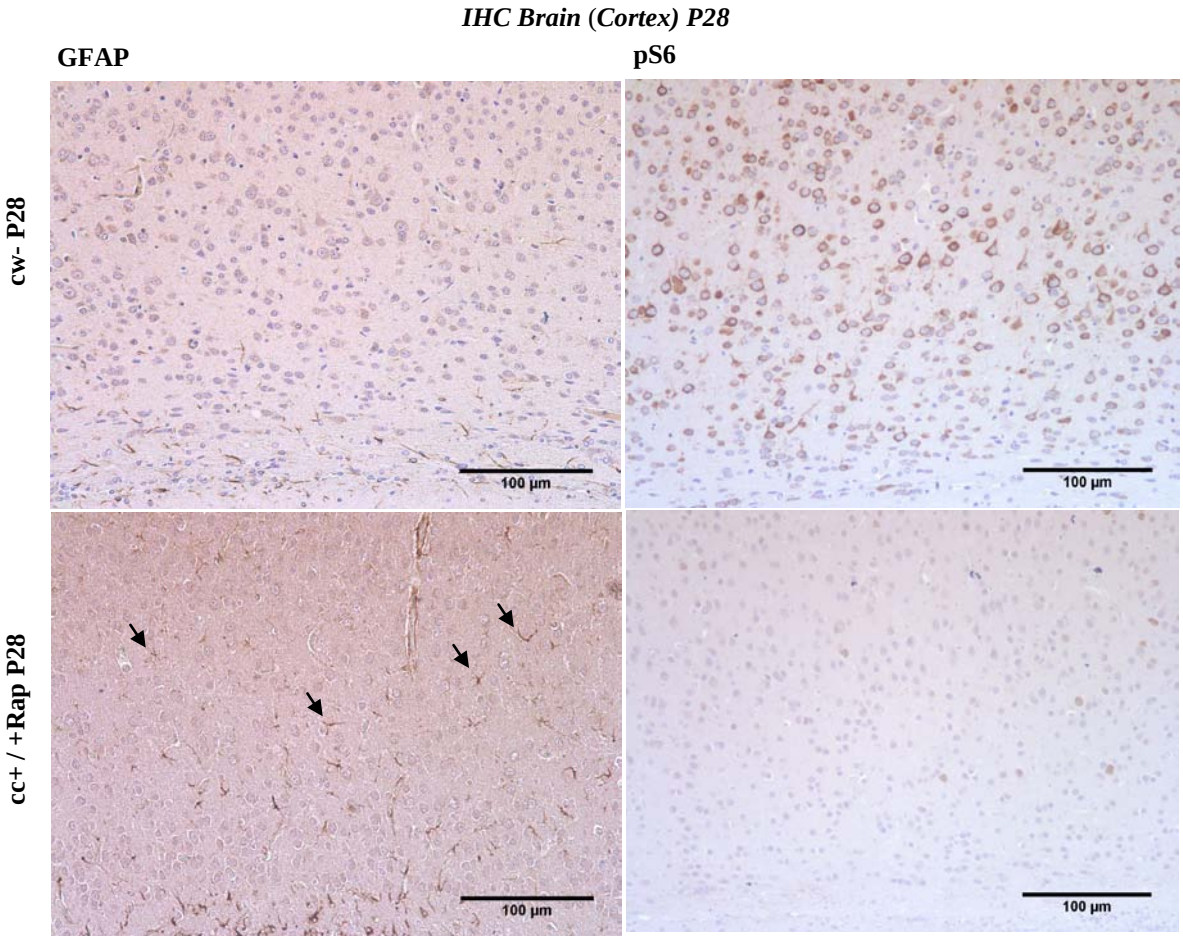

Figure 20: GFAP and pS6 immunohistochemistry of cortex of one control and one mutant at P28 showing astrogliosis in the mutant and striking down regulation of the mTOR pathway due to rapamycin treatment indicated by negative pS6 staining [n=1 (cw^+), n=1(cc^+)].

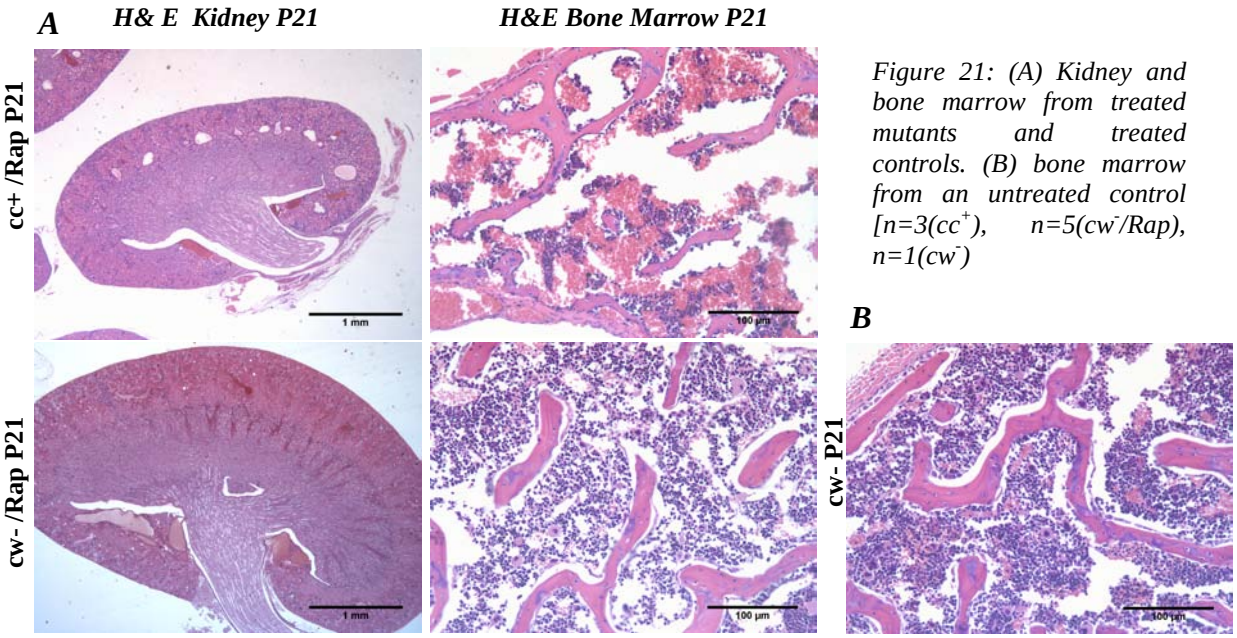

Figure 21: (A) Kidney and bone marrow from treated mutants and treated controls. (B) bone marrow from an untreated control [n=3(cc^+), n=5(cw^-/Rap), n=1(cw^-)

3.6.3 Side effects of Rapamycin treatment

As also seen in newborn mice of all genotypes, the main side effect of rapamycin was a decrease in body weight (figure 10). Even control mice treated by the same treatment schedule (figure 3) and further treated after P21 every other day with 3 mg/kg rapamycin up to the age of 58 days showed decreased body weight compared to untreated controls (figure 16). Another possible side effect of rapamycin treatment seemed to be the delayed eye opening as this feature was seen in some of treated control animals as well (data not shown). Usually eye opening in wild type mice occurs around day 13 which in treated controls shifts to day 16-19 and can vary between fully closed to half open. Five out of eight treated controls showed delayed eye opening during development. In mutant mice the timing of eye opening was even later and closed eyes were seen up to 28 days.

Given the described possible rapamycin side effects, we assumed that we administered an overdose of rapamycin as mTOR activation was drastically suppressed in brain and rapamycin given intraperitoneally may also affect every other organ system. However as seen in figure 21 and 22, rapamycin treatment did not affect the structure and amount of blood progenitor cells in the bone marrow and had no effect on kidney or overall brain structures.

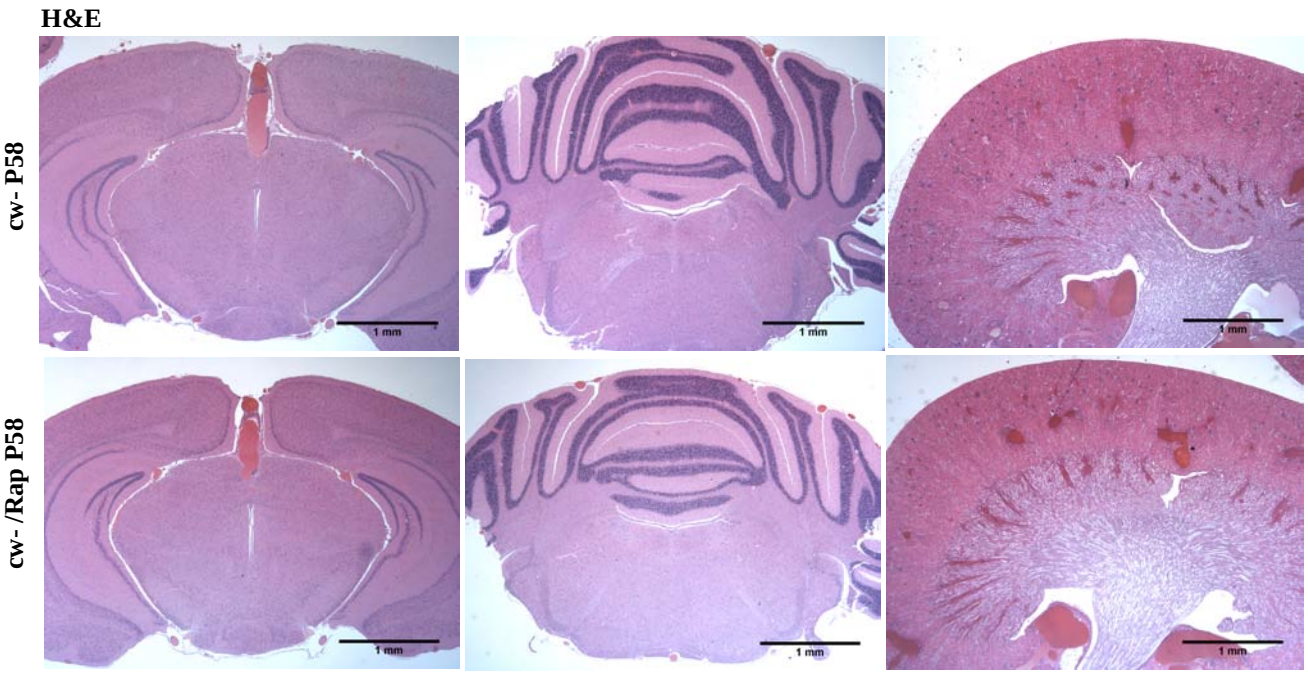

Figure 22: brains and kidneys from treated and untreated controls at P58 showing no side effects of Rapamycin [n=3(cw-/Rap), n=2(cw-)]

3.6.4 Control mice and dose effect of *Tsc1* recombination

As mentioned before, control mice heterozygous for the Nes-Cre (cw^+) allele were used as control for the P0 experiments. Because heterocygosity may also result in a phenotypic manifestation, *cw+* animals were observed by tracking weight and fertility during development. Body weights were monitored at different ages and resulted in a significant reduction in body weight of cw^+ animals. However, viability and fertility and overall condition were not affected. Therefore those animals were used for breeding as well as control animals especially in P0 experiments.

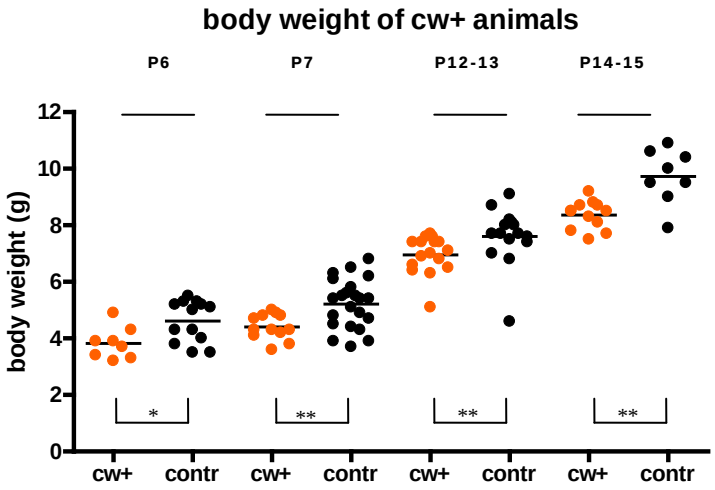

Figure 23: Body weight data from animals heterozygous for the Nes-Cre allele (cw^+). Genotypes of control mice are either cw^- or cc^-; both genders are included

4 DISCUSSION & FUTURE PERSPECTIVES

4.1 Breeding

Initially generation of mutant mice was performed by mating *Tsc1*^{cc} *Nes-Cre*$^{-}$ females with *Tsc1*^{cw} *Nes-Cre*$^{+}$ males. This originally mating strategy yielded only 25% of pups having the desired genotype (*Tsc1*^{cc} *Nes-Cre*$^{+}$) and was both expensive and inefficient, requiring larger numbers of breeding cages. Therefore the breeding was changed to increase the yield of mutants. For this purpose, MLPA analysis was used to determine homozygosity at the Cre allele in males and females. Homozygous Nes-Cre males and females were generated and mated with *cc*$^{-}$ counterparts to generate 1:1 ratio of mutant offspring. One concern using the new breeding scheme was that control animals from the same litter are heterozygous for Nes-Cre. Although we saw a median reduction of body weight only in older *cw*$^{+}$ animals we think that the usage of those animals as controls is adequate, because the animals are viable and fertile. Especially for the P0 experiments *cw*$^{+}$ animals would appear to be suitable controls as body weight reduction is more obvious later in development (figure 23). In addition, it was confirmed that maternally and paternally inherited Nes-Cre allele does not make a difference in survival, phenotype and protein analysis of *Tsc1*^{cc} *Nes-Cre*$^{+}$ offspring (data not shown).

4.2 Pre- and postnatal Rapamycin treatment in a severe mouse model for tuberous sclerosis

Since the *Tsc1*^{cc} *Nes-Cre*$^{+}$ mouse model turned out to have a severe phenotype, causing perinatal death, this novel mutant model could not be used for studying the development of tuber-like brain pathology as seen in TSC patients, as they require a longer survival periods. One approach for the use of this animal model for TSC was to perform a prenatal drug trail. Extensive recombination and loss of *Tsc1* in the brain and associated mTOR activation makes rapamycin the drug of first choice, particularly given the success of this treatment in previous neuronal TSC mouse models. In addition, rapamycin has been described in those mouse brain models as leading to marked improvement. (MEIKLE et al., 2008; ZENG et al., 2008; WOODRUM et al., 2010).

In this mouse model survival of mutant pups was significantly increased with a single dose of rapamycin (1 mg/kg – s.c.) given to pregnant mothers. We showed that rapamycin given to the lactating mother (6 mg/kg – i.p.) between three and seven days after birth leads to transmission of the drug to the offspring with rapamycin brain tissue levels within therapeutic range. However, this treatment did not appear to improve the survival of the offspring compared to mutant groups that received one prenatal dose only (figure 9). Although it has been reported that treatment of female mice with rapamycin (1.5 mg/kg daily for 12 days) impaired mammary gland differentiation and milk protein synthesis (JANKIEWICZ et al., 2006), in our treatment schedule mice received only a single dose at prenatal time points between E11-E18 and therefore should be tolerated much better. We hypothesized that a pre- and perinatal treatment in combination might be too stressful for the mothers as they are in general more sensitive to stressful events during pregnancy and lactation. Any disturbance can easily impact the care and behavior toward the litter. To reduce the stress on the mothers we decided not to continue giving injections during lactation. Whereas one prenatal dose of rapamycin could extend the life span of mutant offspring, the combination of prenatal treatment of the mother and postnatal treatment of the pups themselves improved the survival rate even more. A median survival rate of 20 days could be reached as seen in figure 14. Different time points of rapamycin treatment during gestation led to variable survival rates of the pups. The best achievements in survival were seen with treatment between E15 and E17 (figure 8B). This allows us to postulate that first, rapamycin given around E16 is best tolerated by the pregnant mothers and second, therapeutic benefit on the embryos is most effective at that time point. However, it is very difficult to distinguish between adverse and beneficial effects on both pups and mother. In addition, the dose and timing of prenatal rapamycin treatment in humans would clearly be different given the vastly different time course of embryogenesis in the two species. Nonetheless, the important proof of principle observed here is that rapamycin treatment during pregnancy in this mouse model leads to a marked improvement in survival and phenotype, with survival going from one day to median 20 days. As rapamycin treatment extensively decreases the activation of mTOR as seen in the western blot analysis for phospho-S6 (figure 18), one possible explanation is that the prolonged survival is connected to the down regulation of mTOR in the brain. Although treated animals survive longer, they still show various phenotypes. Most obvious phenotype of rapamycin treated animals is the severe lack of weight gain. Reduction of body weight after rapamycin treatment has been previously shown in other animals models (TAO et al., 2005, CHANG et al, 2010).

Decrease of body weight was shown in newborn mice after prenatal rapamycin treatment as well as in postnatally treated control mice. Another definite side effect is the delayed eye opening seen in treated mice. Whereas eye opening usually occurs around postnatal day 13 it is shifted back to day 16-19 in treated controls and up to day 28 in treated mutants. In more than 60% of the treated controls this phenomenon was seen and may be an additional effect of rapamycin treatment. However, it is also possible that significant growth delay is due to the loss of *Tsc1* in the brain. At that point it is impossible to distinguish between the effect of Tsc1 loss and rapamycin treatment therapy, since untreated mice die soon after birth. It remains open if we can reduce the dose of rapamycin further to avoid the side effects shown here. Additional experiments using reduced doses of rapamycin to further avoid potential side effects need to be performed to answer these open questions in detail.

Since brain histology of treated *Tsc1*^{cc} *Nes-Cre*$^{+}$ mice is restricted to one animal at P28 and therefore it is hard to draw any meaningful conclusions. There may be some features that could not be reversed by rapamycin such as a thicker cortex as seen in the treated animal. More results are available from western blot analysis in which we see gliosis in cortical tissue and a hypomyelination in P21 but not in P28 animals (figure 13A). This suggests a delayed myelination that can be adjusted later on in development. Occurrence of gliosis was confirmed at P28 with immunohistochemistry (figure 20) in which a proliferation of astrocytes is seen throughout the cortex.

Rapamycin does not have any obvious effects on the histological structures of the brain and kidney and as seen in long term treated control animals (figure 22).

We still have no explanation for why treated mutants show relatively severe lack of blood progenitor cells in the bone marrow. A side effect of rapamycin can be excluded as treated control mice show the same status of the bone marrow as untreated controls. Also no recombination in blood building organs could be identified in E16 and P2 lacZ staining (figure 6, 7). Prenatal blood production takes place in the liver, and we saw no evidence (not even single cells) of recombination in the liver. In the postnatal bone marrow recombination of *Tsc1* was not be shown either. It is most likely that a secondary effect takes place due to dysregulation downstream effectors of mTOR in other tissues that are integrated in blood production, such as the kidney which is the main source of erythropoietin.

4.3 Characterization of the *Nes-Cre*$^{+}$ mouse model at P0

In this mouse model in which *Tsc1* is conditionally eliminated in nearly all neuronal progenitor cells, mutant mice die perinatally, show bigger brains and enlarged neurons in the cortex at P0. Those phenotypes are likely to be due to strongly activated mTOR pathway after *Tsc1* loss in neuronal progenitor cells which leads to increased growth and protein synthesis in the brain. Although other organs of *Tsc1* recombination have been detected, no severe lesions have been found in other tissues. Mild structural abnormalities in the brain are seen in the cortex where laminar organization tends to be less distinct in the mutants. Also light disorganization in the hippocampus formation was seen. Abnormal hippocampus formation is associated with the development of seizures in patients with temporal lobe epilepsy which is attended by neuronal loss and gliosis (DICHTER, 2009). We are uncertain if newborn *Tsc1*^{cc} *Nes-Cre*$^{+}$ suffer from seizures. There was no clinical evidence of this (i.e. observed seizures) and electrode placement for electroencephalographic recordings is not possible at that age. In the brain, the majority of the cells show recombination (figure 6), but surprisingly we do not see evidence of this by immunohistochemistry for mTOR activation. Only a subset of cells in the cortical layer V and VI show highly increased levels of pS6 protein, which indicates mTOR activation. In addition, these cells seem to be ectopic and have giant cell character. The evidence suggests that the loss of *Tsc1* occurs in all progenitor cells, but that obvious morphologic effect are seen in only a subset of neurons that may be highly dependent on balanced mTOR activation for some functional reasons. Further studies are required here.

Other brain areas such as hippocampus, cerebellum and brainstem show similar amounts of pS6 positive cells in mutants and controls. Preliminary data suggested a higher amount of pS6 positive cells in a subset of deeper nuclei in the thalamus which are thought to be part of septal nuclei. Septal nuclei are described to be important in linking hypothalamic and brainstem centers with the telencephalon and are the most likely relay stations for communication between somatic and autonomic systems (STAIGER and NÜRNBERGER, 1991). Dysfunction of these circuitries due to *Tsc1* loss and mTOR activation could be a reason of the early death of these mice. However, this is only a hypothesis.

Western blot analysis of whole brain lysates from newborn mice confirmed the high activation of mTOR indicated by elevated phospho-S6 levels and the decline in pAKT activation. S6-kinase is thought to be positively activated in Tsc1 null cells, which induces phosphorylation and

degradation of IRS-1 leading to negative feedback towards (SHAH et al., 2004). Surprisingly, the IRS-1 levels are slightly higher in mutants than in controls which can not be explained so far.

Overall the findings in this model are consistent with previous observations, in that loss of Tsc using a GFAP-promoter driven Cre leads to clinical features and death by 3 months of age (ZENG et al., 2010), and loss of Tsc1 in neuronal cells with the synapsin promoter around E12.5 (MEIKLE et al., 2007) leads to death by 40 days of age. So the much stronger phenotype seen in these mice is consistent with these past models.

Hypotheses and mechanisms that are thought to play a role in the pathogenesis of *Tsc1*^{cc} *Nes-Cre*$^{+}$ mice are discussed in 'future perspectives'.

4.4 Impact of prenatal Rapamycin on *Nes-Cre*$^{+}$ mice at P0

As seen in the studies on P0 pups one dose of rapamycin at E16 is not enough to reverse histological and morphological phenotypes that are seen in untreated pups. Within those is the overall brain size, as well as the brain to body ratio and the size of neuronal cell in cortical layer V and VI. However, protein analysis by western blot showed that one prenatal dose of rapamycin is enough to decrease extensive activation of mTOR and lower the levels of phospho-S6 protein, one of the major downstream effectors of mTOR. This reduction of mTOR activity is thought to be one reason why the survival was significantly increased in *Tsc1*^{cc} *Nes-Cre*$^{+}$ mice. Immunohistochemistry of the cortex showed that prenatal rapamycin treatment leads to a reduction of ectopic and pS6 positive neurons in cortical layers V and VI. Whereas rapamycin is able to block direct effects of mTOR activation, indirect pathway circuits were less affected. Surprisingly protein analysis

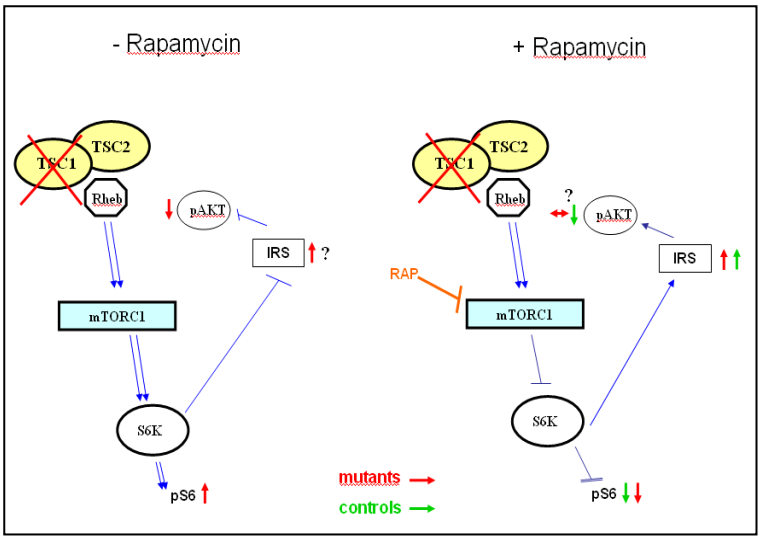

Figure 24: Pathway analysis from P0 brain lysates before and after treatment

showed the same level of pAKT after rapamycin treatment in mutants and decreased pAKT levels in controls. According to the general understanding of the effect of rapamycin on the mTOR pathway, the pAKT levels are thought to increase after treatment, which is a result of decreased S6K activity and leads to a shutdown of the negative feedback loop to AKT functioning via IRS and PI3K. As seen in figure 1 AKT is not only an upstream regulator of mTORC1 but also phosphorylated and activated by mTORC2 and acts there as a downstream effector in cell proliferation and survival.

Although mTORC2 is known not to be sensitive to rapamycin it has been shown that in several cell lines prolonged rapamycin treatment reduces the level of mTORC2 assembly below those needed to maintain AKT signaling. Before the aggregation of the two distinct mTOR complexes newly synthesized mTOR molecules are free in the cytoplasm and can be integrated in both complexes. Therefore long-term exposure to rapamycin can lead to the binding of FKBP12-rapamycin complex to a large fraction of the mTOR molecules in the cell. This event can lead to selective depletion of mTORC2 complex levels, leading to blockade of AKT activation (SARBASSOV et al. 2006). Although this is a possible mechanism, it seems unlikely with a single prenatal treatment in *Tsc1*^{cc} *Nes-Cre*$^{+}$ mice. We suspect, alternatively, that the partial blockade of mTORC1 by a single dose of rapamycin is not sufficient to block the feedback loop that causes relative inactivation of AKT.

4.5 Advantages and Disadvantages of the *Nes-Cre+* mouse model

The early death of the mutant mice represents a major limitation of this mouse model. It is not possible to investigate and generate pathologies seen in patients and the early death makes it difficult to compare this mouse model to other models. Capturing the animals short after within a day is a challenge and often the untreated mutants are already dead, especially when time mating was not efficient as it was the case in this project. Also the perinatal death makes in impossible to compare treated and untreated animals at older ages. Since the whole organism is still under development, the morphology, structure and functions of organs are different and not comparable to adult mice. Also pathway activation may be different. Despite rapamycin treatment mutant mice are very fragile and small and hard to maintain which makes it a time consuming mission to generate animal numbers for statistically significant results. Furthermore, the survival of mutant pups also depends on external factors including the mothering behavior of the mother. It often happens that mothers eat up their pups, which can be stress related or due to behavior defects in

the pups. However, it is remarkable that rapamycin extends the life span of *Tsc1^{cc} Nes-Cre^{+}* animals significantly. This model is usable for investigating the impact of prenatal rapamycin treatment on a severe model of TSC. Further investigation could lead to a better understanding about the relevance of Tsc1 and mTOR signaling in neuronal progenitor cells.

Still the basic characterization of this mouse model has not been completed and the detailed mechanism of death and survival is not understood. No severe lesion could be found in the histology of brain and other tissues that have the potential to cause death. Given the high recombination rate in the central nervous system, it is highly possible that some important neuronal tracks are affected in a way that was not detected by our analysis. Moderate to light variations in basic brain functions can lead to misbehavior or dysfunction of important vital functions that can affect the strength and growth of the pups themselves but also the balance between mother and offspring interaction. Our main hypothesis postulates that brain areas connected to breathing could be affected by recombination of *Tsc1* in the central nervous system. Although this model is termed as brain specific, the leakiness of nestin driven Cre-recombinase is visible by beta-Gal staining, which indicates other tissues and organs also have *Tsc1* recombination. The question remains in what extend those other tissues contribute to the phenotype of *Tsc1^{cc} Nes-Cre^{+}* mice.

4.6 Future Perspectives and planned experiments

4.6.1 Dosage, Timing and Effectiveness of Rapamycin treatment

As seen in the western blot for P21 and P28 animals, rapamycin causes a significant reduction of pS6 levels and consequently inhibits the mTOR pathway. However, the pS6 levels in treated mutants are even lower than in the control animals suggesting an overdose of rapamycin and an adverse effect on the animals due to complete suppression of the mTOR pathway. This could also be a reason for why treated *Tsc1^{cc} Nes-Cre^{+}* animals show such a major growth and weight gain delay. Clearly, further investigations are needed to adapt the dosage of rapamycin to reach a proper balance in mTOR inhibition and activation to keep side effects as low as possible but to accomplish an adequate therapeutic value. However, at this time, it is uncertain whether a lower dose would lead to a better outcome for these mice.

In the Syn1Cre mouse model, rapamycin treatment was started at the age of P7 with a dose of 6 mg/kg (i.p.) every other day up to the age of 100 days. However, it was learned that the dose was

too high causing diarrhea in the pups and poor weight gain. The median survival of 30 days in untreated *Tsc1cc SynCre*$^{+}$ mice could be significantly increased by rapamycin treatment. Because of these observations, we reduced the dosage of rapamyicn to 1 and 3 mg/kg for postnatal treatment and still we achieved a therapeutic effect. Nevertheless we were still concerned that we were over-treating the mice, as protein analysis showed a drastic decline in mTOR activation even lower than in controls. Since mTOR is involved in many crucial cell mechanisms, it is likely to be disadvantageous to block mTOR activity completely by rapamycin treatment especially in pre- and postnatal development.

An important issue for the future usage of rapamycin in TSC fetuses is to adapt the dosage of rapamycin to reach best therapeutic value with lowest side effects. Especially for the prenatal use of rapamycin further studies are needed to be done to exclude possible impacts on the embryo. In the mouse model described here, so far the abortion rate is below 3% of all treated pregnant mothers. This clearly indicates that this single low dose or rapamycin is well tolerated in mice. However, abortion is only the most severe outcome that could result from prenatal rapamycin. Other more subtle effects on growth and development are also extremely important. Notably, we observed that treated pups, both controls and mutants had around 18% lower body weight at birth that untreated pups, suggesting a significant side effect from this treatment Therapeutic effects definitely have to outweigh possible side effects considering prenatal treatment in patients.

One of the planned experiments concerning the dosage we had planned, but were unable to carry out during the thesis interval was, to investigate how long rapamycin lasts in the neonatal mouse and has the desired effect. Protein analysis 4 days after the first postnatal treatment was planned, which is just before the second postnatal treatment. It is possible that giving rapamycin postnatally at either lower dosage or a longer interval might give an improved therapeutic effect. However, analysis of this is time-consuming and expensive as there are many parameters that might be changed.

4.6.2 Breathing abnormalities in newborn mutant mice

Even though the newborn *Tsc1*^{cc} *Nes-Cre*$^{+}$ mice were observed to breathe and be pink on the day of birth, we hypothesize that recombination of *Tsc1* in brain areas critical for important vital functions in the brainstem could be affected and lead to the early death of the animals. Several nuclei and neurons in the brain have been described as being involved in breathing. Those nuclei

can function as CO_2 sensitive chemoreceptors, as pulse generators or are part of the complex signaling network of breathing circuits.

We hypothesize that rapamycin treatment leads to improvement of a possible dysfunction of breathing but cannot reverse the phenotype completely. Treated mutants around 20 days of age that were sacrificed in CO_2 were able to survive much longer than their control litter mates. Although we did not have the opportunity to perform quantitative measurements, it was observed that the mutant mice were resistant to CO^2 exposure, and survived about twice as long as control mice under that same conditions of CO^2 narcosis (e.g. more than 4 minutes vs. 2 minutes). We suggest that they suffer from a mild but chronic breathing dysfunction leads to a chronic hypoxic state. This could explain the finding that those animals when sacrificed with CO_2 showed respiratory function twice as long as control mice. To verify this suggestion we are planning to measure pCO_2 levels as well as bicarbonate and chloride levels that would clarify the status of hypoxia in these animals.

Serotoneric neurons (5-HT neurons) are embedded within the brainstem respiratory network and are thought to play diverse roles, like providing tonic modulatory input in the respiratory network and as CO_2/ pH chemoreceptors. 5-HT neurons, located in the raphé obscurus nucleus project directly to the rhythm-generating pre-Bötzinger complex and respiratory motor neurons. Hodges et al. present a mouse model lacking the Lmx1b transcription factor, which is essential for the development of serotoneric neurons. Neonatal mice lacking selectively the 5-HT neurons display frequent and severe apnea and a decrease in ventilation to less than half of normal. These respiratory abnormalities were most severe during the postnatal period and caused a high perinatal mortality. The surviving animals showed a delay in growth but the respiratory dysfunction faded by the time, pointing out the fact that 5-HT neurons seems to be important in early development. Improvement of apnea indices with a $5\text{-}HT_{2A}$ agonist suggests that the mice have proper developed neuronal network but lack sufficient excitatory input from 5-HT neurons (HODGES et al., 2009).

The regulation of breathing is known to be different in sleep and wake state, which let to the hypothesis that variation in ventilation during sleep could cause perinatal death in *Tsc1*^{cc} *Nes-Cre*$^{+}$ mice when the first period of sleep is reached.

Phox2b is a transcription factor that is essential for the development of visceral reflex circuits It was shown to play a role in the control of breathing as the identification of mutations has been

associated with Central Congenital Hypoventilation Syndrome (CCHS). CCHS is a rare disease defined by the lack of CO_2 responsiveness and of breathing automaticity during sleep. Mice, heterozygous for a common mutation found in CCHS do not respond to hypercapnia and die within the first hour after birth from central apnoea. In these mice the retrotrapezoid nucleus and the parafacial nucleus were found to be severely reduced. These neurons were described as important for regulating proper breathing at birth by chemoreception and the generation of breathing rhythm (AMIEL et al., 2009).

Therefore a planned experiment on *Tsc1*^{cc} *Nes-Cre*$^{+}$ newborn mice is first a whole body plethysmorgaphy, which is used to measure ventilation activity dependent on pressure changes in a chamber system. This would be the first step to prove if breathing is actually involved in the pathology seen in mutant mice. Second if respiratory dysfunction could be measured by a staining with *Phox2b* and serotonin antibodies will be helpful to define breathing related nuclei and analyze possible expression abnormalities of these important regulators of breathing.

Another point to consider is that sleep disturbances are common in TSC individuals, including children. The causes are not certain, but likely to include night-time seizures (KWIATKOWSKI, WHITTENMORE and THIELE, 2010). The question remains if breathing abnormalities could contribute to this and brings up a further reason to think about the breathing center as being involved in this model.

4.6.3 mTOR and Hif-1 alpha

The mTOR pathway has various downstream effectors and is involved in different mechanisms important for maintaining cell homeostasis. Hypoxia-inducible factor 1α (Hif-1α) has been described being integrated in mTOR downstream signaling (figure 25A). Hif-1α is a key factor in mediating gene transcription connected to hypoxic conditions such as the stimulation of erythropoesis, anti-apoptosis, apoptosis, necrosis and angiogenesis by interacting with p53 and VEGF (FAN et al. 2009). There have been several reports that Hif-1α is sensitive to rapamycin, indicating that Hif-1α expression is dependent on mTORC1. Tumors that form as a result of

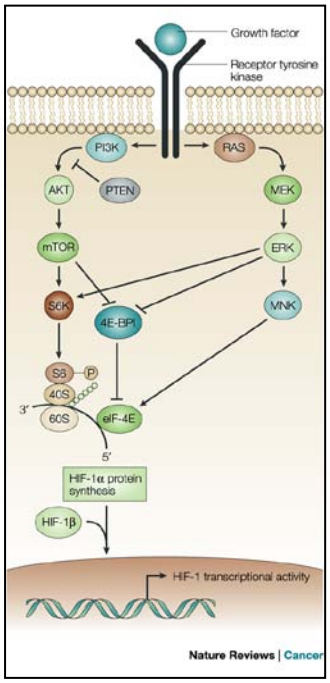

Figure 25: (A) downstream activation of Hif-1α by mTORC1 (Semenza 2003). (B) Hif-1α and its potential to regulate cell surbival as well as apoptosis (Fan et al., 2006)

increased mTOR signaling have highly vascularization which is induced by Hif-1α. mTOR inhibition with rapamycin can diminish the angiogenesis. So the activation of mTOR enhances the activity of Hif-1α and the secretion of vascular endothelial growth factor (VGFE)-A during hypoxia (LAND et al., 2007). During normal oxygen conditions Hif-1α is rapidly degraded by ubiqutination and degradation targeted to the proteasome. Due to its short half life of only several minutes it is hardly detectable under normoxic circumstances. Therefore transcriptional activities of Hif-1α target genes are also inhibited. Hypoxia leads to an immediate shutdown of general protein translation and to decreased energy consumption. Activation of MAP-Kinase due to

hypoxia phosphorylates and stabilizes Hif-1α which acts on promoter regions of several hypoxia responsive genes.

In a study of neonatal hypoxic-ischemic brain injury it has been shown that the induction of apoptosis by Hif-1α is dependent on the severity of hypoxia. Under mild hypoxic conditions transcriptional activation mainly promote cell survival by erythropoesis, angiogenesis and anti-apoptosis. During severe hypoxia, the transcriptional activation mainly leads to cell necrosis and apoptosis induced p53 and other related transcription factors (figure 25B) (FAN et al., 2009). In cancer treatment rapamycin is used to inhibit the mTOR downstream effector Hif-1α, which leads to inhibition of the interaction between VEGF and VEGF-Receptor to suppress angiogenesis and tumor growth. Crucial questions for the *Tsc1*^{cc} *Nes-Cre*$^{+}$ mouse model is if highly activated mTOR leads to expression of Hif-1α and induces severe hypoxia pathway as shown in figure 25B which is connected with cell death and could lead to the death of the mice. With Rapamycin treatment the Hif-1α activation could be down regulated and the mild hypoxia pathway may lead to survival of cells and the whole organism. However, apoptotic cells in the brain of newborn untreated *Tsc1*^{cc} *Nes-Cre*$^{+}$ animals could not be seen so far.

Nevertheless it is from certain interest to investigate the expression status from mTOR downstream genes and proteins in *Tsc1*^{cc} *Nes-Cre*$^{+}$ to get more insight into the development of pathogenesis in this mouse model.

4.6.4 Blood tests

A deficit of precursor blood cells in the bone marrow of treated mutants at the age of 21 and 28 days respectively led to the hypothesis that anemia occurred as a side effect of rapamycin treatment or in consequence of other *Tsc1* recombination sites due to Nes-Cre expression. The first presumption could be disproved as treated control animals show normal bone marrow comparable to untreated control animals. No recombination was found in blood building organs, neither in the embryonic liver where blood production takes place before birth nor in the bone marrow of mice after birth at P2. As the kidney is the major site of recombination after the central nervous system the idea came up that peritubular cells in the kidney that are responsible for erythropoietin synthesis could be somehow affected and cause imbalance of erythropoietin release and signaling between kidney and bone marrow. However, blood cell counting in newborn mice demonstrated only a slight decrease in white and red blood cell numbers (RBC, WBC) and no severe signs of anemia that would cause death could be detected. In contrast,

hematocrit (HCT) and hemoglobin values are significantly higher in mutant animals at P0 whereas red blood cell numbers (RBC) are the same. This would suggest an increase in red blood cell size. Higher HCT without an increase of blood cells is found if an organism is dehydrated. This seems unlikely in the P0 mutant pups, as they show milk in the gut and do not seem to be dehydrated due to starvation. The opposite observation was found in rapamycin treated pups. Whereas WBC and RBC are higher, the HCT is lower. WBC numbers are not thought to decrease with rapamycin treatment but a shift in cell population occurs which induces the immunosuppressive effect (CHEN et al., 2010). Why total WBC numbers increase in *Tsc1*^{cc} *Nes-Cre*$^{+}$ mice remains unclear. Also uncertain remains the HCT value which is decreased in both treated controls and mutants.

Further plans include blood tests on P0 pups, especially for glucose as the most obvious trend is seen here and mTOR signaling has recently been associated with the regulation of glycolysis & gluconeogenesis, fatty acid synthesis and the pentose phosphate pathway (ZHANG et al., 2009, HOUDE et al., 2010).

4.6.5 Behavioral studies

Since TSC in patients is often have neurodevelopmental features like mental retardation and autism spectrum disorders, it is of interest to see if rapamycin can have both positive and negative effects on behavior and learning. For these reasons behavioral studies on wild type animals are planned that got pre- and postnatal rapamycin treated or a placebo treatment. Basic behavioral studies will include rotarod, elevated plus maze, and the open field test. The rotarod test involves a rodent being placed on a horizontally oriented, rotating cylinder that accelerates. The animals naturally try to stay on the rotarod to avoid falling to the ground. The length of time that an animal stays on the rotarod is an indicator of their balance and coordination and is used to define basic motor functions. Also the test can be used to define learning progress when performed in a sequence of several days. The elevated plus maze is commonly used to assess anxiety-like behaviour. It consists of an elevated maze with two open arms and two closed arms. The test aims at quantifying the natural conflict between rodents fear of open spaces versus their exploratory behaviour. Elevated anxiety is indicated with prolonged stay in the closed arms. Open field studies are used to measure locomotor activity, hyperactivity, and exploratory behaviours.

4.7 Impact of Rapamycin on *Nes-Cre+* mice and therapeutic values for patients

The most important conclusion resulting from this project is that prenatal rapamycin can at least partly reverse a severe phenotype that is caused by depletion of *Tsc1* in the brain and cause a significant improvement in survival. Fortunately, this severe phenotype is seen very rarely in TSC patients, as complete loss of either *Tsc1* or *Tsc2* is thought to occur after a second hit in only a very small subset of cells, which then give rise to tubers and subependymal nodules. Nonetheless, as tubers develop early in gestation and can be detected by ultrasound analysis it is of potential interest to consider prenatal or early postnatal administration of rapamycin or related drug. The results presented here show that prenatal rapamycin treatment is tolerated in a severe mouse model for TSC brain disease and is beneficial for the survival of animals that are affected by loss of Tsc1 in the brain. Further studies are needed to confirm that rapamycin has no or minimal impact during embryonic and infantile development which essential when thinking of this treatment approach in people. Also a main subject in which more work has to be done is the choice of dose to reach maximize therapeutic benefit while minimizing possible side effects.

All in all these preliminary data are the first step in considering prenatal rapamycin treatment to improve disease progression and health related quality of life in TSC patients.

5 ZUSAMMENFASSUNG

Tuberöse Sklerose (TS) ist eine autosomal-dominant vererbte Krankheit, die mit einer Inzidenz von 1 in 6000 Geburten auftritt und eine komplexe Systemerkrankung darstellt. Tumorartige Veränderungen können in mehreren Organsystemen auftreten wobei Gehirn, Haut, Niere, Herz und Lunge besonders betroffen sind. Als Ursache für die Erkrankung hat man genomische Veränderungen sowie große Deletionen, Insertionen, missense und nonsense Mutationen in den Genen *TSC1* und/oder *TSC2* gefunden. *TSC1* und *TSC2* kodieren für die Proteine Hamartin beziehungsweise Tuberin, die eine Schlüsselfunktion in der Regulierung des mTOR (mammalian Target of Rapamycin) Signalwegs haben. Dieser Signalweg spielt eine wichtige Rolle in Proteinsynthese und Zellwachstum, in Abhängigkeit von Wachstumsfaktoren und Nährstoffen und wurde mit der Entstehung von Tumoren bei Fehlregulation in Verbindung gebracht. Die Verwendung von Maus Modellen hat große Fortschritte im Verständnis von der Entstehung und den grundlegenden molekularen Mechanismen von tuberöser Sklerose geführt. Mehrere Mausmodelle für die Untersuchung von Gehirnpathologien in TSC wurden generiert, wobei keines dieser Modelle kortikale glioneuronale Hamartome (Tubera), die die häufigste Pathologie in TSC Patienten ist, entwickelt.

In dieser Studie wird ein konditionaler Knockout Stamm untersucht und vorgestellt in dem man mit Hilfe vom Nestin-Promoter, einem Promoter spezifisch für Neuroprogenitorzellen, das *Tsc1* Gen gewebespezifisch in neuronalen Vorläuferzellen unter Verwendung von Cre-Rekombinase ausschaltet. Die Rekombination von *Tsc1* konnte im Zentralnervensystem und Nieren sowie in einzelnen Zellen von Lunge und Herz nachgewiesen werden. Der Verlust von *Tsc1* führt zu einer konstitutiven Aktivierung des mTOR Signalwegs in den betroffenen Zellen und Geweben und außerdem zu perinataler mortalität von mutanten Tieren. Ursprünglich sollte dieses Modell dazu verwendet werden, die Manifestation von TSC im Gehirn zu untersuchen und ein Maus Modell für kortikale glioneuronale Harmatome zu entwickeln. Da Mutanten dieses Stammes (*Tsc1*^{cc} *Nes-Cre*$^{+}$) aber perinatal sterben, liegt der Schwerpunkt in diesem Projekt auf pre- und postnataler Verabreichung von Rapamycin und dessen Wirkung auf Schwangerschaft und Überlebensrate der betroffenen Tiere. Rapamycin ist ein fungaler Metabolit, der weitläufig als Immunsupressivum besonders bei Transplantat-Patienten eingesetzt wird und außerdem seine Wirkung als Inhibitor vom oben beschriebenen mTOR Signalwegs darstellt. Die positive Wirkung von Rapamycin wurde bereits in mehreren Studien an Maus Modellen für TSC gezeigt.

Ein Teil der Arbeit besteht aus der allgemeinen Charakterisierung des Maus Modells an neugeborenen Tieren. Mutanten entwickeln größere Gehirne und zeigen eine Erhöhung des phospho-S6 (pS6) Proteins im Gehirn, ein *downstream effector* des mTOR Siganlwegs, der als Indikator für mTOR Aktivität verwendet wird. Durch eine pränatale Dosis von 1mg/kg Rapamycin konnte das pS6 Level deutlich reduziert werden. Das Verhältnis von Gehirn und Körpergewicht ist bei Mutanten um 20% höher als bei Kontrolltieren. Dieses Merkmal kann durch eine pränatale Dosis von Rapamycin nicht reversiert werden, dennoch kann die Überlebensrate signifikant gesteigert werden. Der genaue molekulare Mechanismus der perinatalen Letalität konnte nicht im Detail gezeigt werden. Es wird vermutet, dass Zentren im Gehirn die wichtige lebenserhaltende Funktionen wie Atem- Lungenfunktion aufrecht erhalten durch die Rekombination von *Tsc1* betroffen sind und zum frühen Tod der mutanten Tiere führen.

Im zweiten Teil der Arbeit wird die Kombination von pre- und postnataler Verabreichung ab dem achten Lebenstag von Rapamycin beschrieben, womit die mittlere Überlebensrate auf 20 Tage gesteigert werden konnte. Die Tiere einen deutlichen Phänotyp zeigen, der durch eine Reduktion im Wachstum, ein verspätetes Öffnen der Augen und Tremor charakterisiert ist, und in histologischen untersuchen milde Gliosis zeigen.

Zusammenfassend kann man sagen, dass Rapamycin in diesem Mausmodell für tuberöse Sklerose, dessen schwerwiegender Phänotyp durch perinatalen Tod gekennzeichnet ist, einen entscheidenden Effekt hat und die Überlebensrate signifikant erhöht. Von Interesse wäre eine pränatale Behandlung von schwangeren Frauen mit Rapamycin, deren Familie bereits eine Vorgeschichte von tuberöser Sklerose hat und bei denen man TSC im ungeborenen Kind diagnostiziert hat. Nichtsdestotrotz sind die Resultate dieser Arbeit vorerst Pilotstudien und man benötigt nicht nur höhere Tierzahlen aber auch genauere Untersuchungen von Dosis und Nebeneffekten von Rapamycin in der embryonalen und infantilen Entwicklung.

6 SUMMARY

Tuberous sclerosis complex (TSC) is an autosomal dominant disorder with an incidence of one in 6000 births, in which multiple organ systems are affected by benign tumors termed hamartomas. Most of the pathology is seen in brain, skin, kidney, heart and lungs. Genomic alterations such as large genomic deletions, rearrangements, insertion and missense and nonsense mutations in the tumor suppressor genes, *TSC1* and/or *TSC2*, have been shown to be responsible for TSC and often lead to a truncated, nonfunctional protein. *TSC1* and *TSC2* encode the proteins Hamartin and Tuberin, respectively, which play a key role in regulation of the mTOR (mammalian Target of Rapamycin) signaling pathway. mTOR is important for protein synthesis and cell growth, depending on the availability of nutrients and growth factors and has been implicated in tumor development.

In recent years, there has been increasing appreciation for the value of TSC mouse models for both understanding disease pathogenesis and therapeutic drug trials. So far several mouse models of TSC brain disease have been developed. However, none of them showed tuber lesions, the most common pathology seen in TSC patients. In this study, a new mouse brain model was generated and described in which *Tsc1* is deleted in brain progenitor cells using a nestin promoter construct to drive expression of cre-recombinase. *Tsc1*^{cc} *Nes-Cre*$^{+}$ mice showed extensive recombination and inactivation of the *Tsc1* gene during brain development, which leads to nearly complete loss of expression of Tsc1 at birth in brain tissues, constitutive activation of mTOR and mortality at one day of age. Originally, this model was generated to establish and investigate glioneuronal hamartomas, the main brain manifestations in TSC. Because of the perinatal death, the emphasis in this project is to investigate the effects and therapeutic values of pre- and postnatal rapamycin treatment and its impact on survival of pups and pregnancy. Rapamycin, a product of the bacterium *Streptomyces hygroscopicus,* is widely used as immunosuppressant, serves as an inhibitor of the mTOR and has been shown to have major benefit in other TSC mouse brain models.

One part of this study covers the basic characterization of the mouse model at birth and the effect of prenatal rapamycin treatment. Mutant mice show enlarged brains and an increase of phospho-S6 (pS6) protein, which is a downstream marker of mTOR and serves as an indicator of mTOR activity. One prenatal dose of 1 mg/kg of rapamycin to the pregnant mother decreased the pS6 levels significantly and improved the survival of mutants. The ratio of brain and body weight was

20% higher in untreated mutants than in controls. Although this feature could not be reversed by prenatal rapamycin treatment, the treated mutants significantly extend their life span. The cause of death at birth has not been determined in detail but is thought to be due to *Tsc1* loss in brainstem areas important for basic life functions such as breathing. In the second part I describe that pre- and postnatal treatment in combination restored the survival of mutant mice up to median survival of 20 days. These animals show an obvious phenotype that includes a reduction in growth, delayed eye opening, tremor and straub tail and show gliosis in brain pathology.

Although caution is appropriate, taken together, these date demonstrate that rapamycin has a significant benefit on the survival of a TSC brain model. These preclinical data in this mouse model suggest that prenatal rapamycin treatment might be beneficial for people with a family history of TSC and were TSC has been diagnosed in an unborn child. However the data shown here are preliminary and needs more investigation on an increased number of animals and on the dosage and effect of rapamycin in embryonic and infant development.

7 REFERENCES

AMIEL J, DUBREUIL V, RAMANANTSOA N, FORTIN G, GALLEGO J, BRUNET JF, GORIDIS C., PHOX2B in respiratory control: lessons from congenital central hypoventilation syndrome and its mouse models.

Respir Physiol Neurobiol. 2009 Aug 31;168(1-2):125-32.

ASTRINIDIS A, HENSKE EP., Tuberous sclerosis complex: linking growth and energy signaling pathways with human disease.

Oncogene. 2005 Nov 14;24(50):7475-81.

BISSLER JJ, McCORMACK FX, YOUNG LR, ELWING JM, CHUCK G, LEONARD JM, SCHMITHORST VJ, LAOR T, BRODY AS, BEAN J, SALISBURY S, FRANZ DN., Sirolimus for angiomyolipoma in tuberous sclerosis complex or lymphangioleiomyomatosis.

N Engl J Med. 2008 Jan 10;358(2):140-51.

CHANG GR, WU YY, CHIU YS, CHEN WY, LIAO JW, HSU HM, CHAO TH, HUNG SW, MAO FC., Long-term administration of rapamycin reduces adiposity, but impairs glucose tolerance in high-fat diet-fed KK/HlJ mice.

Basic Clin Pharmacol Toxicol. 2009 Sep;105(3):188-98.

CHEN JF, GAO J, ZHANG D, WANG ZH, ZHU JY., CD4+Foxp3+ regulatory T cells converted by rapamycin from peripheral CD4+CD25(-) naive T cells display more potent regulatory ability in vitro.

Chin Med J. 2010 Apr 5;123(7):942-8.

CRINO PB, NATHANSON KL, HENSKE EP., The Tuberous Sclerosis Complex

N Engl J Med. 2006 Sep 28; 355(13):1345-56.

DAHLSTRAND J, LARDELLI M, LENDAHL U., Nestin mRNA expression correlates with the central nervous system progenitor cell state in many, but not all, regions of developing central nervous system.

Brain Res Dev Brain Res. 1995 Jan 14;84(1):109-29.

DICHER MA., Emerging concepts in the pathogenesis of epilepsy and epileptogenesis.

Arch Neurol. 2009 Apr;66(4):443-7.

DUBOIS NC, HOFMANN D, KALOULIS K, BISHOP JM, TRUMPP A., Nestin-Cre transgenic mouse line Nes-Cre1 mediates highly efficient Cre/loxP mediated recombination in the nervous system, kidney, and somite-derived tissues.

Genesis. 2006 Aug;44(8):355-60.

EHINGER D, HAN S, SHILYANSKY C, ZHOU Y, LI W, KWIATKOWSKI DJ, RAMESH V, SILVA AJ., Reversal of learning deficits in a Tsc2+/- mouse model of tuberous sclerosis

Nat Med. 2008 Aug;14(8):843-8.

EKER R., Familial renal adenomas in Wistar rats; a preliminary report.

Acta Pathol Microbiol Scand. 1954;34(6):554-62.

FAN X, HEINJEN CJ, van der KOOIJ MA, GROENENDAAL F, van BEL F., The role and regulation of hypoxia-inducible factor-1alpha expression in brain development and neonatal hypoxic-ischemic brain injury.

Brain Res Rev. 2009 Dec 11;62(1):99-108.

FRANZ DN, LEONARD J, TUDOR C, CHUCK G, CARE M, SETHURAMAN G, DINOPULOS A, THOMAS G, CRONE KR., Rapamycin causes regression of astrocytomas in tuberous sclerosis complex.

Ann Neurol. 2006 Mar;59(3):490-8.

HASTY P.; Rapamycin: the cure for all that ails

J Mol Cell Biol. 2010 Feb;2(1):17-9.

HENGSTSCHLÄGER M., Tuberous sclerosis complex genes: from flies to human genetics.

Arch Dermatol Res. 2001 Aug; 293(8):383-6.

HOUDE VP, BRULE S, FESTUCCIA WT, BLANCHARD PG, BELLMANN K, DESHAIES Y, MARETTE A., Chronic rapamycin treatment causes glucose intolerance and hyperlipidemia by upregulating hepatic gluconeogenesis and impairing lipid deposition in adipose tissue.

Diabetes. 2010 Jun;59(6):1338-48.

INOKI K, GUAN KL., Tuberous sclerosis complex, implication from a rare genetic disease to a common cancer treatment

Hum Mol Genet. 2009 Apr 15;18(R1):R94-100.

INOKI K, CORRADETTI MN, GUAN KL., Dysregulation of the TSC-mTOR pathway in human disease.

Nat Genet. 2005 Jan;37(1):19-24.

INOKI K, ZHU T, GUAN KL., TSC2 mediates cellular energy response to control cell growth and survival.

Cell. 2003 Nov 26;115(5):577-90.

INOKI K, LI Y, ZHU T, WU J, GUAN KL., TSC2 is phosphorylated and inhibited by Akt and suppresses mTOR signalling.

Nat Cell Biol. 2002 Sep;4(9):648-57.

JANKIEWICZ M, GRONER B, DESRIVIERES S., Mammalian target of rapamycin regulates the growth of mammary epithelial cells through the inhibitor of deoxyribonucleic acid binding Id1 and their functional differentiation through Id2.

Mol Endocrinol. 2006 Oct;20(10):2369-81.

KENERSON HL, AICHER LD, TRUE LD, YEUNG RS., mammalian target of rapamycin pathway in the pathogenesis of tuberous sclerosis complex renal tumors.

Cancer Res. 2002 Oct 15;62(20):5645-50.

KNOWLES MA, PLATT FM, ROSS RL, HURST CD., Phophatidylinositol 3-kinase (PI3K) pathway activation in bladder cancer

Cancer Metastasis Rev. 2009 Dec;28(3-4):305-16.

KOBAYASHI T, MINOWA O, KUNO J, MITANI H, HINO O, NODA T., Renal carcinogenesis, hepatic hemangiomatosis, and embryonic lethality caused by a germ-line Tsc2 mutation in mice.

Cancer Res. 1999 Mar 15;59(6):1206-11.

KOBAYASHI T, MINOWA O, SUGITANI Y, TAKAI S, MITANI H, KOBAYASHI E, NODA T, HINO O., A germ-line Tsc1 mutation causes tumor development and embryonic lethality that are similar, but not identical to, those caused by Tsc2 mutation in mice.

Proc Natl Acad Sci U S A. 2001 Jul 17;98(15):8762-7.

KOZLOWSKI P, LIN M, MEIKLE L, KWIATKOWSKI DJ., Robust method for distinguishing heterozygous from homocygous transgenic alleles by multiplex ligation-dependent probe assay

BioTechniques 2007 May;42(5):584-588

KWIATKOWSKI DJ, WHITTENMMORE HV, THIELE EA, Tuberous Sclerosis Complex; Genes, Clinical Features and Therapeutics

1. Edition, April 2010

KWIATKOWSKI DJ, MANNING BD, Tuberous sclerosis: a GAP at the crossroads of multiple signaling pathways.

Hum Mol Genet. 2005 Oct 15;14 Spec No. 2:R251-8.

KWIATKOWSKI DJ., Tuberous sclerosis: from tubers to mTOR.

Ann Hum Genet. 2003 Jan;67(Pt 1):87-96.

KWIATKOWSKI DJ., Rhebbing up mTOR: new insights on TSC1 and TSC2, and the pathogenesis of tuberous sclerosis.

Cancer Biol Ther. 2003 Sep-Oct;2(5):471-6.

KWIATKOWSKI DJ, ZHANG H, BANDURA JL, HEIBERGER KM, GLOGAUER M, el-HASHEMITE N, ONDA H., A mouse model of TSC1 reveals sex-dependent lethality from liver hemangiomas, and up-regulation of p70S6 kinase activity in Tsc1 null cells

Hum Mol Genet, 2002 Mar1:11(5):525-34

LAND SC and TEE AR., Hypoxia-inducible factor 1alpha is regulated by the mammalian target of rapamycin (mTOR) via an mTOR signaling motif.

J Biol Chem. 2007 Jul 13;282(28):20534-43.

LANGKAU N, MARTIN N, BRANDT R, ZÜGGE K, QUAST S, WIEGELE G, JAUCH A, REHM M, KUHL A, MACK-VETTER M, ZIMMERHACKL LB, JANSSEN B., and TSC2 mutations in tuberous sclerosis, the associated phenotypes and a model to explain observed TSC1/ TSC2 frequency ratios.

Eur J Pediatr. 2002 Jul;161(7):393-402.

LAW BK., Rapamycin: an anti-cancer immunosuppressant?

Crit Rev Oncol Hematol. 2005 Oct;56(1):47-60.

MANNING BD, TEE AR, LOGSON MN, BLENIS J, CANTLEY LC., Identification of the tuberous sclerosis complex-2 tumor suppressor gene product tuberin as a target of the phosphoinositide 3-kinase/akt pathway.

Mol Cell. 2002 Jul;10(1):151-62.

MEIKLE L, TALOS DM, ONDA H, POLLIZZI K, ROTENBERG A, SAHIN M, JENSEN FE, KWIATKOWSKI DJ., A mouse model of tuberous sclerosis: neuronal loss of Tsc1 causes dysplastic and ectopic neurons, reduced myelination, seizure activity, and limited survival.

J Neurosci. 2007 May 23;27(21):5546-58.

MEIKLE L, POLLIZZI K, EGNOR A, KRAMVIS I, LANE H, SAHIN M, KWIATKOWSKI DJ., Response of a neuronal model of tuberous sclerosis to mammalian target of rapamycin (mTOR) inhibitors: effects on mTORC1 and Akt signaling lead to improved survival and function.

J Neurosci. 2008 May 21;28(21):5422-32.

MERIC-BERNSTAM F and GONZALEZ-ANGULO AM, Targeting the mTOR Signaling Network for Cancer Therapy

J Clinic Oncol., May 1, 2009; 27(13):2278-2287

ONDA H, LUECK A, MARKS PW, WARREN HB, KWIATKOWSKI DJ., Tsc2(+/-) mice develop tumors in multiple sites that express gelsolin and are influenced by genetic background

J Clin Invest. 1999 Sep;104(6):687-95.

PAUNESKU T, MITTAL S, PROTIC M, ORYHON J, KOROLEV SV, JOACHIMIAK A, WOLOSCHAK GE.; Proliferating cell nuclear antigen (PCNA): ringmaster of genome

Int J Radiat Biol. 2001 Oct;77(10):1007-21.

PAXINOS G, HALLIDAY G, WATSON C, KOUTCHEROV Y, WANG HQ; Atlas of the Devloping Mouse Brain at E17.5, P0, and P6

First Edition, 2007; Copyright © 2007 Elsevier Inc.

SHAH OJ, WANG Z, HUNTER T., Inappropriate activation of the TSC/Rheb/mTOR/S6K cassette induces IRS1/2 depletion, insulin resistance, and cell survival deficiencies.

Curr Biol. 2004 Sep 21;14(18):1650-6.

SARBASSOV DD, ALI SM, SENGUPTA S, SHEEN JH, HSU PP, BAGLEY AF, MARKHARD AL, SABATINI DM., Prolonged rapamycin treatment inhibits mTORC2 assembly and Akt/PKB.

Mol Cell. 2006 Apr 21;22(2):159-68.

SAUER B., Inducible gene targeting in mice using the Cre/lox system

Methods. 1998 Apr;14(4):381-92.

SAUER B, HENDERSON N., Site-specific DNA recombination in mammalian cells by the Cre recombinase of bacteriophage P1.

Proc Natl Acad Sci U S A. 1988 Jul;85(14):5166-70.

SEMENZA GL, Targeting HIF-1 for cancer therapy

Nat Rev Cancer 3, 2003 Oct:3(10):10-721-732

SHACKELFORD DB, VASQUEZ DS, CORBEIL J, WU S, LEBLANC M, WU CL, VERA DR, SHAW RJ., mTOR and HIF-1alpha-mediated tumor metabolism in an LKB1 mouse model of Peutz-Jeghers syndrome.

Proc Natl Acad Sci U S A. 2009 Jul 7;106(27):11137-42.

STAIGER JF and NÜRNBERGER F., The efferent connections of the lateral septal nucleus in the guinea pig: projections to the diencephalon and brainstem.

Cell Tissue Res. 1991 Jun;264(3):391-413.

SORIANO P. 1999. Generalized lacZ expression with the ROSA26 Cre reporter strain

Nat Genet Jan 21(1):70-1.

SOULARD A, HALL MN., SnapShot: mTOR signaling.

Cell. 2007 Apr 20;129(2):434.

TAO Y, KIM J, SCHRIER RW, EDELSTEIN CL., Rapamycin markedly slows disease progression in a rat model of polycystic kidney disease.

J Am Soc Nephrol. 2005 Jan;16(1):46-51.

TEPPERMAN E, RAMZY D, PRODGER J, SHESHGIRI R, BADIWALA M, ROSS H, RAOA V., Surgical biology for the clinician: vascular effects of immunosuppression.

Can J Surg. 2010 Feb;53(1):57-63.

TRONCHE F; KELLENDONK C; KRETZ O; GASS P; ANLAG K; ORBAN PC; BOCK R; KLEIN R; SCHUTZ G. 1999. Disruption of the glucocorticoid receptor gene in the nervous system results in reduced anxiety.

Nat Genet 23(1):99-103.

UHLMANN EJ, WONG M, BALDWIN RL, BAJENARU ML, ONDA H, KWIATKOWSKI DJ, YAMADA K, GUTMANN DH., Astrocyte-specific TSC1 conditional knockout mice exhibit abnormal neuronal organization and seizures.

Ann Neurol. 2002 Sep;52(3):285-96.

VEZINA C, KUDELSKI A, SEHGAL SN.; Rapamycin (AY-22,989), a new antifungal antibiotic. I. Taxonomy of the producing streptomycete and isolation of the active principle.

J Antibiot (Tokyo). 1975 Oct;28(10):721-6.

VALERO J., WERUAGA E., MURIAS A.R, PORTEOS A, ALONSO J.R., Immunodetection of BrdU and PCNA in the rostral migratory stream of the adult mouse

Current Issues on Multisdisciplinary Microscopy Research and Education, pages 118-129, FORMATEX Microscopy Book Series (N°2)

WATANABE N, HIRAMATSU K, MIYAMOTO R, YASUDA K, SUZUKI N, OSHIMA N, KIYONARI H, SHIBA D, NISHIO S, MOCHIZUKI T, YOKOYAMA T, MARUYAMA S, MATSUO S, WAKAMATSU Y, HASHIMOTO H., A murine model of neonatal diabetes mellitus in Glis3-deficient mice.

FEBS Lett. 2009 Jun 18;583(12):2108-13.

WONG M, ESS KC, UHLMANN EJ, JANSEN LA, LI W, CRINO PB, MENNERICK S, YAMADA KA, GUTMANN DH., Impaired glial glutamate transport in a mouse tuberous sclerosis epilepsy model.

Ann Neurol. 2003 Aug;54(2):251-6.

WOODRUM C, NOBIL A, DABORA SL., Comparison of three rapamycin dosing schedules in A/J Tsc2+/- mice and improved survival with angiogenesis inhibitor or asparaginase treatment in mice with subcutaneous tuberous sclerosis related tumors.

J Transl Med. 2010 Feb 10;8:14.

ZHANG HH, HUANG J, DÜVEL K, BOBACK B, WU S, SQUILLACE RM, WU CL, MANNING BD., Insulin stimulates adipogenesis through the Akt-TSC2-mTORC1 pathway.

PLoS One. 2009 Jul 10;4(7):e6189.

ZHOU J, BRUGAROLAS J, PARADA LF., of Tsc1, but not Pten, in renal tubular cells causes polycystic kidney disease by activating mTORC1.

Hum Mol Genet. 2009 Nov 15;18(22):4428-41

ZENG LH, XU L, GUTMANN DH, WONG M., Rapamycin prevents epilepsy in a mouse model of tuberous sclerosis complex.

Ann Neurol. 2008 Apr;63(4):444-53.

ZENG LH, BERO AW, ZHANG B, HOLTZMAN DM, WONG M., Modulation of astrocyte glutamate transporters decreases seizures in a mouse model of Tuberous Sclerosis Complex

Neurobiol Dis. 2010 Mar;37(3):764-71.

WEB PAGES:

Tuberous Sclerosis Alliance, http://www.tsclinic.org;

Jackson Laboratories, http://cre.jax.org/Nes/Nes-Cre.html, http://cre.jax.org/introduction.

8 ABBREVIATIONS

bp	base pairs
E	embryonic day
mTOR	mammalian Target of Rapamycin
mAB	monoclonal Antibody
pAB	polyclonal Antibody
TSC	Tuberous Sclerosis Complex
P0	postnatal day zero/ birthday (equals E19)
P1, P2,..	postnatal day one, two,..
µm	micrometer

9 ACKNOWLEGDEMENTS

First I want to thank David J Kwiatkowski, MD, PhD for giving me the opportunity to join his research group at Brigham and Woman's Hospital which was a great abroad experience for me to improve my technical and language skills. Furthermore he taught me precious knowledge in planning and arranging scientific projects. My acknowledgement goes to him and the Austrian Marshallplan Foundation for financial support that made the project accomplishable.

My special thanks go to June Goto, PhD who supervised me with patience, accuracy and kindness throughout the whole year of my stay. She taught and helped me to perform and plan all my practical experiments and supported me in realizing my thesis. Also outside the lab she was a great companion. I want to thank all other members of the Kwiatkowski-Lab for their cooperativeness in all kind of situations in the lab. The nice atmosphere made it a pleasure to work.

In addition I want to thank all cooperating people who are mentioned below who contributed in great extent to the project with important results, theories and advices.

I want to thank A. Prof. Dr. rer.nat. Marina Karaghiosoff who provided her support as an internal supervisor within the University of Veterinary Medicine Vienna.

Last but not least I want to thank my family and friends back in Vienna who supported me despite the distance and my great roommates and friends here in Boston who I can always count on.

10 COOPERATIONS

Harvard Medical School / Rodent Histopathology Core

Roderick T. Bronson, D.V.M

Childrens Hostpital Boston / Behavioral Studies

Mustafa Sahin, MD, PhD

Abbey Sadowski

Dana-Farber Cancer Institute / Blood Tests

Yoji Andrew Minamishima, MD, PhD

Harvard Medical School / Sequencing Core

Mei-Huang Lin, chief technician